COMPARATIVE IMAGING OF SURGICAL SMALL INTESTINAL DISEASE IN DOGS: EVALUATION OF PRE-OPERATIVE CONTRAST-ENHANCED ULTRASOUND, INTRA-OPERATIVE CONTRAST-ENHANCED ULTRASOUND, AND TRIPLE-PHASE CONTRAST-ENHANCED COMPUTED TOMOGRAPHY

BY

ELISABETH F. PETERS GOODALL

THESIS

Submitted in partial fulfillment of the requirements
for the degree of Master of Science in VMS - Veterinary Clinical Medicine
in the Graduate College of the
University of Illinois at Urbana-Champaign, 2016

Urbana, Illinois

Master's Committee:

Assistant Professor Heidi Phillips, Chair
Clinical Assistant Professor Jodi S. Matheson
Professor Emeritus Matthew A. Wallig

ABSTRACT

Surgical small intestinal diseases occur commonly in canine patients seen in veterinary practices. Failure to identify ischemic tissue intra-operatively can result in surgical dehiscence, require surgical revision, and lead to sepsis or death. Currently contrast-enhanced computed tomography (CT) is the standard of care for evaluating ischemic lesions of the bowel in humans. Contrast-enhanced ultrasound (CEUS) is an alternative method for evaluating tissue perfusion whose utility for evaluation of canine small intestinal lesions remains to be fully tested. Thirteen client-owned dogs were prospectively recruited after presenting with surgical diseases within the small intestine. Presenting conditions included discrete foreign bodies, linear foreign bodies, intestinal abscess, and neoplasia. Patients underwent pre-operative CEUS, triple-phase contrast-enhanced CT, and intra-operative CEUS. Surgical specimens obtained from each patient included resected intestinal segments or biopsy. Both CT and CEUS data were compared to histopathology findings. All patients that required a resection (n=4) received an ischemia score of 4 or 5. A higher ischemia score was correlated with an increased chance of necrosis (p=0.003) and thrombosis (p=0.024). The presence of a visual perfusion deficit on CT was correlated with a higher ischemia grade (p=0.048) and higher chance of necrosis (p=0.024); however, observers only detected a perfusion deficit in 3/4 (75%) of patients requiring a resection. Ischemia was correlated with lower Hounsfield (HU) values aborad to the lesion in the pre-contrast CT (p=0.049). Necrosis was correlated with increased HU values at normal intestine in the arterial phase (p=0.017) and orad to the lesion in the venous phase of CT (p=0.014). Thrombosis was correlated with lower HU values aborad to the lesion in the pre-contrast CT (p=0.025) and higher HU values at normal intestine in the arterial phase (p=0.037) and orad to the lesion in the venous phase CT (p=0.041). Edema was correlated with lower HU values aborad to the lesion in the arterial phase (p=0.03) and higher HU values at normal intestine in the venous phase CT (p=0.038). Ulceration and erosion were correlated with higher HU values orad to the lesion in both the arterial (p=0.028) and venous phases of CT (p=0.044). No significant correlations were found at the site of the lesion in any phase of CT. For pre-operative CEUS, edema was correlated with higher peak intensity

(p=0.014) while necrosis (p=0.046) and thrombosis (p=0.04) were correlated with a faster time to peak. For intra-operative CEUS, ulceration and erosion were correlated with a greater inflow slope (p=0.045), hemorrhage was correlated with a longer time to initial rise (p=0.028), thrombosis was correlated with a faster time to peak (p=0.014), and necrosis was correlated with increased baseline pixel intensity (p=0.046). Observers were able to detect a perfusion deficit on CEUS exam in 4/4 (100%) of patients requiring a resection. No advantage to the intra-operative CEUS versus a pre-operative CEUS exam was appreciated. Lower HU values obtained from the pre-contrast CT aborad to the lesion site (p=0.036) and at normal intestine (p=0.036) were correlated with a higher chance of patient mortality. The presence of a visual perfusion deficit on CEUS was also correlated with a higher chance of patient mortality (p=0.014). Findings from our study indicate that a variety of CT and CEUS findings were correlated with various histopathologic features, with no single imaging modality found to be superior. The clinical application of these findings warrants further investigation.

TABLE OF CONTENTS

CHAPTER 1

REVIEW OF THE LITERATURE

Contrast ultrasound agents:

Contrast ultrasound agents were initially used as a tool in echocardiography. They provided a way to delineate tissue margins, evaluate for vascular shunting, and characterize regurgitant cardiac valvular lesions.[1,2] The contrast agents did this by improving the signal-to-noise ratio, as they provide a strongly echogenic interface between gas and liquid or tissue,[3] and therefore increased the echogenicity of blood.[4] As blood moved through the cardiovascular system, its path could also be traced based on the location of contrast injection and its flow evaluated for any abnormalities.

Intravascular free gas bubbles, such as those created in agitated saline, were one of the first contrast ultrasound agents used, and are still used today.[5] One of its downfalls is that the bubbles created are a variety of sizes and are prone to coalescing into larger bubbles.[1] These larger gas bubbles could be potentially harmful within the vascular system of a patient, particularly when trapped within the pulmonary vascular system, resulting in air embolism. The high variability of bubble size also poses a challenge to reproducing a consistent contrast effect.[4] Another issue is that the number of individual bubbles declines rapidly once administered due to this coalescing behavior. Therefore their echogenic contrast capabilities also diminish rapidly.[1] To combat these problems, efforts were made to stabilize these bubbles using products such as indocyanine green dye, lipid emulsions, dextrose, or sorbitol.[1,2,4] Attempts were also made at using intravascular injections of compounds which created microbubbles *in vivo*, such as dilute hydrogen peroxide or a combination of sodium bicarbonate and ascorbic acid.[1] Eventually the idea of forming a stabilized wall around the gas bubble was developed. This stabilized wall could be comprised of gelatin, lipid, or albumin.[1,2] The concept of a central gas bubble surrounded by a protective shell eventually lead to the formation of the contrast agents used today.

A variety of modern-day microbubble contrast agents are available, all comprised of a gas encapsulated in a stabilized, thin shell which is often comprised of phospholipids.[3] These require the use of harmonic or pulse-inversion imaging techniques.[6] Currently, only 2 agents, Optison™ (GE Healthcare, Buckinghamshire, UK) and Definity® (Lantheus Medical Imaging, North Billerica, MA) are FDA-approved within the United States and their labeled use is restricted to cardiac imaging.[7] Some agents remain intravascular, while others have prolonged enhancement with an arterial, portal venous, and parenchymal phase. The parenchymal phase is associated with imaging of the liver and spleen, as these contrast agents are taken up by the reticuloendothelial system within the hepatic and splenic parenchyma.[8] To combat some of the problems associated with previous ultrasound contrast agents, microbubbles are extremely small in size, many in the 2-5μm range, which is smaller than the diameter of a red blood cell. This smaller size allows the microbubbles to cross capillary beds and undergo recirculation within the vascular system for a prolonged period of time (minutes) prior to rupturing.[3] The shell components are eliminated by the liver and spleen, and the inert gas is eliminated by exhalation through the lungs.[9] These agents can also be administered either as a rapid bolus or as a continuous rate infusion to further prolong the length of enhancement.[3] One study also evaluated methods for prolonging contrast enhancement while under general anesthesia. It was found that in rats, medical grade air as the isoflurane carrier instead of pure oxygen, lengthened the circulation of microbubbles.[10]

Contrast-enhanced ultrasound (CEUS) has evolved into a method of evaluating tissue perfusion both in subjective real-time assessment and in post-exam image analysis. A specific region of interest (ROI) can be drawn within a target site and from this specific perfusion parameters can be calculated to create a time intensity curve.[11] These measurements can then be used clinically to assess perfusion of an organ or lesion. The ROI should be drawn as close to the level of the focal zone as possible and, if performing multiple ROIs within a sample, ROIs should be as close to the same depth of field as possible.[12]

Overall safety and risk of adverse reaction to modern-day contrast ultrasound agents has also been evaluated both in human and veterinary medicine. A large retrospective study evaluating Definity® and Optison™ administration in human medicine found their safety to be excellent. This multicenter study evaluated 78,383 doses (66,164 doses of Definity®, 12,219 doses of Optison™) administered over a course of 6.5 years for imaging evaluation ranging from routine outpatient echocardiography procedures to inpatient procedures performed in critically ill intensive care unit patients. Both cardiac and abdominal imaging uses were reported. No deaths were reported and no patients who experienced adverse events required hospitalization or observation for longer than 4-8 hours after the reaction. A total of eight reactions were probably related to the contrast study, two reactions were possibly related to the contrast study, and 6 reactions were considered unlikely to be related to the contrast study. For the eight reactions most likely associated with contrast use, all patients received Definity®. Four of these patients experienced severe anaphylactic reactions which occurred in less than 15 minutes after contrast injection and all responded to antihistamines, steroids, fluids, and/or epinephrine. Two patients experienced urticaria and lip swelling which occurred in less than 30 minutes after contrast injection and both responded to antihistamines. One patient experienced a vasovagal response characterized by dizziness and nausea which occurred within 1 minute after contrast administration and responded to fluids. One patient experienced acute hypoxemia which occurred within 1 minute after contrast administration and responded to a bronchodilator. No adverse events occurred in the critically ill intensive care unit patients or in those presenting for acute chest pain. Over 10,000 contrast doses were administered to this high risk population. The overall risk of adverse reaction was 0.006% for Definity® and 0% for Optison™ for this study population.[13]

In the largest retrospective veterinary study performed to date, 488 animals, 411 dogs and 77 cats, were evaluated for frequency and type of adverse reaction following the use of CEUS. Compared to the 262 control cases which had standard B-mode ultrasound performed, the risk of death within 24 hours of the procedure was not significantly different between groups. No cats which had CEUS performed exhibited

either immediate or delayed reactions. 3 dogs exhibited immediate reactions (vomiting or syncope) and 1 dog exhibited a delayed reaction (vomiting), with an overall prevalence of adverse events of 0.2% for dogs.[14]

Advantages of CEUS are the lack of nephrotoxicity from the contrast agents themselves and the absent risk of ionizing radiation, both of which are considerations prior to using other advanced imaging modalities.[7]

Contrast-enhanced ultrasound in human medicine:

As the original application of contrast ultrasound agents was for use in cardiac imaging, it is logical that cardiac and vascular imaging remains one of the most widely investigated areas of contrast ultrasound. A common use for CEUS is for evaluation of myocardial perfusion, particularly during episodes of suspected acute myocardial infarction.[4,15,16] This is achieved by direct injection of a contrast agent into the left ventricle or the coronary arteries themselves or by peripheral intravenous injection. Rapid detection of acute myocardial infarction in symptomatic patients can not only aid in defining the myocardial area at risk, but may also help define optimal treatment. In cases where there are smaller contrast defects, a more conservative approach is necessary. Treatment is aimed at restoring flow in the affected coronary artery, however cases have shown that even after return of artery flow, microvascular reperfusion can be lacking in up to 23% of cases.[15] CEUS can help detect this vascular and microvascular changes, to better predict patients who will be predisposed to recovery complications. Other forms of vascular imaging investigated include characterization of carotid body tumors[17], identification of carotid plaque vascularization[18], detection of cervical arterial dissection or arterial aneurysms, and diagnosis of inflammatory vasculopathies.[19]

Another research area in which CEUS has been widely utilized is for the detection and characterization of hepatic neoplasia. Numerous studies have focused on characterizing focal hepatic lesions as benign or malignant pre-operatively.[20–25] In one study, malignant lesions were much more frequently found to be hypoenhancing or non-enhancing in the last phase (91% of malignant lesions vs. 37% of benign lesions). In a small percentage of the study population that had benign lesions, hyperenhancement was noted in the late phase (20% of benign lesions). This enhancement pattern was not seen in any of the malignant lesions. To the contrary, hyperenhancement was noted in the early phase in 20% of malignant lesions and only in 2% of benign lesions. Overall this yielded a sensitivity of 90%, specificity of 99% and accuracy of 89% for determination of malignant focal hepatic lesions.[22] A study which specifically examined the characteristics of focal fatty infiltration of the liver also demonstrated unique perfusion patterns in benign hepatic nodules. This disease can appear nodular and be difficult to distinguish from malignant liver nodules. They found the focal fatty infiltrative lesions were hypo- or isoenhancing during the arterial phase and isoenhancing during the portal venous and delayed phases.[21]

One study found that the perfusion characteristics on contrast ultrasound correlated well with the histological differentiation of hepatocellular carcinoma (HCC). Four distinct perfusion patterns were noted: normal, cotton, vascular, and dead wood. A normal perfusion pattern demonstrated indistinct margins between the tumoral tissue and normal tissue, with tumor perfusion similar to surrounding normal hepatic parenchyma. The cotton pattern had a well-defined border between tumoral and normal issue, but the tumor vasculature was indistinct and overall the tumoral area appeared hypoperfusing. A normal or cotton perfusion pattern was associated with a very well-differentiated HCC. In the vascular pattern, tortuous tumor vessels were clearly noted. A vascular pattern was associated with a moderately differentiated HCC. The dead wood pattern also noted distinct tumor vessels, but they were more sparse, tapered and were abruptly terminating, giving an overall heterogeneous enhancement appearance. A dead wood pattern was associated with a poorly differentiated HCC.[26]

CEUS has been used to aid in the diagnosis of hepatic fibrosis. For this analysis, the hepatic vein transit time (extrahepatic vascular component) and the hepatic transit time (intrahepatic vascular component) were assessed with CEUS. Transit times were found to be shorter in patients with hepatic fibrosis compared to normal. Both transit time measurements were reliable and accurate for this purpose, and were beneficial to add a non-invasive tool in the diagnosis of this disease.[27]

Perfusion characteristics of hepatic lipidosis conditions have also been described. Specifically, non-alcoholic steatohepatitis (NASH) was found to appear significantly different on CEUS compared to non-alcoholic fatty liver disease. For patients with NASH, contrast enhancement was significantly decreased. This study used the contrast agent Levovist and was able to establish a cut-off intensity value at 43.6 at 20 minutes post-injection. Using this established cut-off point, the sensitivity, specificity, and accuracy of distinguishing NASH patients among patients with fatty liver disease were 100%.[28]

Intra-operative use of CEUS in human medicine is mainly reserved for evaluation of liver nodules for criteria of malignancy. While intra-operative ultrasound is commonly used for detection of metastatic liver nodules during surgery[29–33], it has been shown that the addition of CEUS to the intra-operative exam may further improve metastatic detection within the liver. One group evaluated patients in which all had undergone computed tomography (CT) imaging of the abdomen as standard pre-operative staging. The addition of standard intra-operative ultrasound (IOUS) evaluation of the liver resulted in detecting additional lesions in 33% of patients. The further addition of intra-operative CEUS changed the diagnosis of 19% of patients. This included characterizing hepatic nodules as benign or malignant based on perfusion characteristics, and having that determination differ from pre-operative assessment. In 1 out of the 21 total patients tested, intra-operative CEUS detected an additional metastatic nodule which was not able to be visualized on CT or standard IOUS. Overall, this study demonstrated the impact intra-operative CEUS can have on patient management.[34]

A study from the same year demonstrated a similar degree of importance in using intra-operative CEUS for oncologic patient management. This study evaluated the utility and safety of intra-operative CEUS in 20 patients undergoing laparotomy for resection and/or ablation of known neoplastic liver lesions. A variety of liver tumors were studied, including metastatic colorectal neoplasia, primary hepatocellular neoplasia, intrahepatic cholangiocarcinoma, metastatic renal neoplasia, and metastatic carcinoid. In many cases additional hepatic lesions were identified and in all cases existing lesions were better delineated with regards to overall lesion size and quality of lesion margination. Based on the evaluation of the CEUS exam, surgical planning was altered in 5/20 patients to obtain appropriate surgical margins. This altered hepatic resection from partial to complete lobectomy in the affected patients. No patients demonstrated adverse reactions or alteration in anesthetic parameters during or after the procedure. Researchers found intra-operative CEUS to be a safe and effective tool for hepatic oncologic surgical planning.[35]

Several musculoskeletal uses of contrast-enhanced ultrasound have also been evaluated. One study evaluated finger joints in rheumatoid arthritis patients to determine whether it could be used as a reliable non-invasive tool to differentiate active disease from those in remission, as neovascularization and overall synovial vascularity correlate with disease activity. Comparing the CEUS in conjunction with color Doppler to a color Doppler exam alone, the addition of a contrast ultrasound agent improved detection of intraarticular neovascularization.[36] In a similar later study, patients with active disease showed consistent contrast enhancement of the synovium compared to those in remission, with an 100% sensitivity and 96% specificity.[37]

Contrast ultrasound has also proven helpful in evaluation of the urogenital tract. A comparative study between contrast-enhanced CT and CEUS for detection of acute pyelonephritis in a subset of patients exhibiting clinical signs consistent with acute pyelonephritis was performed. Contrast-enhanced CT is considered the imaging method of choice for this disease process in humans. Of the 100 patients

included, CT detected renal changes consistent with acute pyelonephritis in 84 of the patients. CEUS detected changes consistent with disease in 82/84 of those patients in which abnormalities were noted on CT. Even with the 2 false negative contrast ultrasound exams, it still proved to be a useful test and may be a viable alternative in which concern for CT radiation exposure or contrast agent safety exist.[38]

In evaluating the genital tract, CEUS has also been shown to be useful. When comparing conventional B-mode ultrasound to contrast ultrasound of the prostate in which hypoechoic foci had already been visualized and proven via biopsy to be neoplastic, B-mode ultrasound underestimated tumor size in 76.67% of lesions and overestimated size in 20% of lesions. CEUS underestimated tumor size in 48.33% of lesions and overestimated size in 26.67% of lesions. On correlation analysis, CEUS correlated strongly (r=0.91) with histopathology measurements, whereas B-mode ultrasound correlated weakly (r=0.59) with histopathology measurements.[39] In cases where distinct prostatic lesions are not visualized by B-mode ultrasound but suspicion for prostatic neoplasia exists based on labwork such as prostate-specific antigen testing, contrast ultrasound can also be performed to help guide biopsy localization.[40] CEUS can also be used to monitor response of prostatic carcinoma to anti-androgen therapy, and correlated well with a decline in prostate specific antigen in patients who responded to treatment.[41] Assessment of prostatic neoplasia using three dimensional contrast-enhanced power Doppler has been performed, but the clinical indications of this imaging method remain unclear.[42] 3-D contrast ultrasound has also been described in women to assess patency of Fallopian tubes.[43] The usefulness of CEUS in distinguishing benign vs malignant ovarian tumors has also been evaluated.[44]

Several studies have evaluated the usefulness of CEUS for diagnosis of intestinal ischemia.[45–48] In one such study, fifty patients were prospectively enrolled after presenting for bowel obstruction. Seventeen patients had intestinal ischemia resulting from either intestinal strangulation, thromboembolism of the superior mesenteric artery, or non-occlusive disease. The remaining thirty-three patients had simple intestinal obstructions. When imaging was performed using contrast-enhanced ultrasound, all patients

with simple intestinal obstructions had normal contrast exams. Only one false negative for intestinal ischemia was noted in a case of bowel strangulation. This yielded excellent sensitivity (94.1%), specificity (100%), positive predictive value (100%) and negative predictive value (97.1%) for the diagnosis of intestinal ischemia using CEUS.[45]

Another group found similarly promising results for the use of CEUS in diagnosing intestinal ischemia. In this study, fifty-one patients presenting with evidence of intestinal dilation on radiographs had CEUS performed. Twenty patients had intestinal ischemia due to either bowel strangulation or thromboembolism of the superior mesenteric artery. The remaining thirty-one patients had simple intestinal obstruction. Focal intestinal CEUS was performed at the most dilated loop of small intestine and signal was classified as normal, diminished, or absent. The majority of patients with intestinal ischemia had absent CEUS signal (12/20). Diminished CEUS signal was found in 5/20 intestinal ischemia cases. Few cases of intestinal ischemia (3/20) and all cases of simple intestinal obstruction (31/31) had normal CEUS signal. When combining the absent and diminished groups as a predictor of intestinal ischemia, CEUS again yielded high sensitivity (85%), specificity (100%), positive predictive value (100%), and negative predictive value (91.2%).[46]

A similar study was performed evaluating the utility of CEUS for the diagnosis of intestinal ischemia. In this study, sixty-five patients were enrolled with a clinical suspicion for intestinal ischemia. 14/65 patients had intestinal ischemia and all had diminished CEUS signal when examined. One case which initially was classified as diminished CEUS signal was ultimately proven to have no evidence of intestinal ischemia. The remaining cases (50/65) had normal CEUS signal and no ultimate evidence of intestinal ischemia. Using a classification of diminished signal intensity on CEUS as a predictor for intestinal ischemia, the resultant sensitivity (100%), specificity (98%), positive predictive value (93%), and negative predictive value (98.5%) were excellent. Overall accuracy of CEUS was 98.5% with 64/65 patients correctly classified as ischemic or non-ischemic intestinal disease.[47]

Researchers are still evaluating and exploring ways in which contrast ultrasound may prove useful. Such areas include determining methods for assessing vascularity of adipose tissue[49] and skeletal muscle.[50] The use of contrast agents which had previously been developed for and used solely in ultrasound, has also been under investigation for use in magnetic resonance imaging. The microbubbles have been demonstrated to have an effect on transverse relaxation times[51,52] and were also shown to alter the signal intensity for spin-echo and gradient-echo pulse sequences.[52] As the contrast microbubbles are pressure sensitive, they may provide a new route of gauging vascular pressure gradients or cardiac chamber pressures[52] or be an alternative method of determining cerebral blood volume.[53]

Researchers are also investigating the utility of contrast ultrasound microbubbles as targeted mechanical transporters within the vascular system. Not only can microbubbles allow for site-specific drug delivery by use of conjugated ligands or monoclonal antibodies, but their efficacy can potentially be further enhanced by rupturing the microbubbles at a specific organ, lesion, or area of interest.[54] This is accomplished by adjusting the acoustic power while focusing the ultrasound transducer on the desired target site.[9] Still, many microbubbles will continue to circulate and be eliminated outside the target site. Benefits of this method, however, are avoiding or minimizing systemic side effects, lowering the effective dose required, and improving the therapeutic efficacy of the drug administered.[55] One area of research uses the surface of microbubbles to transport ligands to endothelial selectins or integrins[56] which allows for active molecular targeting to a target site. This method of microbubble drug-loading is referred to as surface loading.[55] These microbubbles may prove useful for allowing targeted drug delivery into the high flow and high shear stress arterial vascular system. They have also been utilized to carry ligands for endothelial cell adhesion molecules expressed during inflammation such as VCAM-1[57] and ICAM-1, which results in microbubbles binding in areas with a high degree of vascular inflammation.[58] Microbubbles have also been coated with antibodies, such as prostate-specific antigen monoclonal antibodies, and proven to be able to target and bind prostatic cancer cells in vitro.[59] These microbubbles

may provide researchers both a novel method of prostatic cancer detection and allow for targeted drug delivery.

In fact, specialized microbubbles have been developed specifically for use with drug delivery. These specialized microbubbles are comprised of multiple layers, with the central gas core surrounding by an oil-drug mixture and coated in a lipid shell containing surface ligands.[60] This method of microbubble drug-loading is known as entire volume loading, as the drug is carried within the shell as opposed to on the surface.[55] Still others have instead approached drug delivery by covalently linking microbubbles which are formed with an albumin shell to nanoparticles, with hopes of using the nanoparticles as drug carriers.[61] These are known as secondary carrier-associated microbubbles.[55]

Several studies have begun evaluating this novel approach to drug delivery with chemotherapeutics. One study is attempting to exploit the transient cell membrane permeability that occurs when microbubbles collapse,[62,63] and has evaluated the internalization of the chemotherapeutic drug cisplatin in multiple carcinoma cell lines *in vitro*. They found cytotoxicity increased in a dose dependent manner as these cisplatin carrying microbubbles were administered. *In vivo* experiments using immunodeficient mice inoculated with carcinoma also showed a reduction in tumor volume in mice treated with the cisplatin microbubbles.[64]

Contrast-enhanced ultrasound in veterinary medicine:

The most prolific area of research for contrast enhanced ultrasound in veterinary medicine involves the liver. In 2003, a group of researchers published their data investigating whether CEUS could help distinguish unique perfusion characteristics in canine patients with single congenital extra-hepatic portosystemic shunts. When analyzing the angiographic changes of the liver, the hepatic arteries

appeared larger and more tortuous. There were also changes noted with general hepatic perfusion. Dogs with a portosystemic shunt demonstrated shorter time to peak intensity and a more rapid contrast inflow.[65]

The same year, a group from the same institution published data from hepatic CEUS in canine patients without evidence of liver disease. This study not only aimed to establish normal hepatic perfusion parameters for standard time intensity values (inflow slope, outflow slope, baseline intensity, peak intensity, time to peak intensity) but also to determine whether a bolus injection or constant-rate infusion of contrast agent was preferable. They found that the two injection methods carried significant differences in almost all parameters evaluated. It was also concluded that the bolus injection method was not only easier, but resulted in improved repeatability of the data and therefore easier data analysis.[66]

Soon afterwards, a review article evaluating the important role of CEUS in human medicine for analyzing metastatic disease of the liver and lymph nodes was published in a veterinary journal. It was noted that this technique could play a role in advancing veterinary diagnostic imaging as well.[67] The investigators later published data analyzing normal canine liver using the bolus injection technique in both awake and anesthetized patients. Time to peak intensity was significantly shorter in anesthetized dogs, but the remaining time intensity values showed no significant difference between groups. Although the overall number of analyzed patients was small (n=11), no abnormalities were noted clinically or in standard laboratory parameters used to evaluate safety.[68]

The first report of the utility of CEUS for evaluation of hepatic nodules was published around this same time period. This study was a landmark for multiple reasons, as it was one of the largest sample populations used to date in veterinary medicine, was the first study evaluating pathologic hepatic changes in dogs, where cytologic or histologic confirmation of pathology was included. Both benign and malignant hepatic nodular lesions were evaluated and many differences were noted. Malignant nodules appeared hypoechoic compared to surrounding hepatic parenchyma at peak enhancement, whereas benign

nodules were isoechoic. Malignant nodules also subjectively appeared more conspicuous than benign nodules. In fact, contrast administration made a larger quantity of nodules apparent for those with malignant lesions. As in previous studies, no adverse reactions were noted among test patients.[69]

A later report confirmed the utility of CEUS for detection of metastatic liver nodules. This report included only 3 patients but had clinically significant findings nonetheless. In all patients, splenic hemangiosarcoma and the normal ultrasonographic appearance of the liver was required. After contrast administration, hypoechoic nodules became apparent within the hepatic parenchyma that could not be otherwise sonographically visualized. These hepatic nodules were later confirmed by histology to be metastatic hemangiosarcoma.[70]

A later study evaluating focal hepatic lesions in dogs used the contrast agent Sonazoid® (Daiichi Pharmaceutical Co., LTD, Tokyo, Japan), which differs from the agents used in previous veterinary studies in that it is taken up by the hepatic reticuloendothelial system and has a true parenchymal enhancement phase. The previously published veterinary studies used agents that remained strictly intravascular. Benign nodules were hyperplastic (nodular hyperplasia or cirrhotic nodules) while malignant nodules consisted of a variety of neoplasms including carcinoma, lymphoma, malignant histiocytosis, mast cell tumor, and various sarcomas. A hypoechoic appearance compared to surrounding parenchyma was again noted to be associated with malignancy. More numerous malignant nodules were also seen in the parenchyma after contrast administration. For those dogs with hepatocellular carcinoma, an initial hypervascular change was noted in the arterial phase (n=5/6) prior to the later hypoechoic appearance (n=4/6). Additional vascular patterns unique to specific neoplasms were not appreciated.[71]

Not long after, a similar study was performed using Sonazoid® in the evaluation of canine liver nodules, using phased imaging (arterial, portal venous, parenchymal). This study again found that the initial arterial phase and the later parenchymal phase were both useful for distinguishing benign from malignant

nodules. Malignant nodules had various echogenicity during the arterial phase, but had consistently different echogenicity compared to the surrounding parenchyma. These nodules again became hypoechoic to surrounding normal liver in the parenchymal phase.[72]

Evaluation of the spleen with CEUS has had more varied results. A study aimed at defining baseline time intensity data for splenic perfusion with CEUS found no significant differences between patient weight, age, gender, or various red blood cell parameters, among other variables. There was rapid visualization of vessels near the splenic hilus, whose branches radiated throughout the parenchyma prior to an overall heterogeneous enhancement of the parenchyma. This initial heterogeneous pattern is important to note, so not to be confused with a pathologic enhancement pattern as seen in other organs. A phase followed this which exhibited homogeneous enhancement followed by a gradual decline in perfusion intensity.[73]

Another study investigating normal splenic perfusion characteristics demonstrated Sonazoid's® long-acting effects on splenic enhancement as a contrast ultrasound agent. Uniform enhancement persisted for 30 minutes, with the ideal time period for splenic analysis between 7-30 minutes after contrast injection. In contrast to other agents used such as Definity® who enhancement capabilities last merely a few minutes, Sonazoid® demonstrated usefulness as a longer-acting agent.[74]

The same group to publish the first data defining CEUS characteristics of normal spleen also was the first to investigate its utility for distinguishing benign and malignant splenic nodules. In this study, a persistently hypoechoic nodule was significantly associated with malignancy. However, if marked hyperechogenicity was observed, this pattern could not distinguish between the two classifications.[75]

A similar study by a different group observed that lesion hypoechogenicity in the parenchymal wash-out phase in conjunction with the visualization of tortuous feeder vessels was associated with splenic malignancy. In addition, certain malignancies revealed unique characteristics. Lymphosarcoma had

rapid wash-in and early wash-out, with a "honeycomb" appearance during the wash-out phase. Hemangiosarcoma appeared to have persistently anechoic (nonperfused) areas within a large mass compared to hyperenhancing splenic parenchyma.[76] In several patients, more numerous nodules were noted within the spleen after contrast administration, similar to previous characteristics of malignant hepatic nodules already described.[69–71] Most of the benign nodules observed appeared similar to surrounding splenic parenchyma in all phases. A single patient also was noted to have an accessory spleen, which showed an identical enhancement pattern as the adjacent spleen.[76]

As CEUS characteristics of malignant splenic nodules were still not clearly defined, Taeymans and Penninck hoped their work might finally find a cohesive thread. Instead of evaluating overall lesion perfusion pattern, they found more reliable results using analysis of the lesion's feeder vessels to help determine malignancy. Malignant splenic nodules were observed to have persistent visualization of tortuous feeder vessels which wrapped around the periphery of the nodule. This finding added yet another layer of potential in defining benign or metastatic splenic lesions, but failed to fully unite with previous studies' findings.[77]

Changes within lymph nodes have also been evaluated to help determine whether malignancy is present. In one study, 11 dogs known to have lymphoma underwent CEUS exam involved lymph nodes. These malignant prescapular and submandibular lymph nodes were found to have more vessels visualized with CEUS than with power Doppler exam.[78] They also appeared homogeneous, with fair to good enhancement, as opposed to hypoenhancing changes noted with other organs when malignant nodules are found.[70–72] Many angioarchitectural characteristics were noted including central hilar vessels and aberrant vessels, but the most common vascular change noted with these malignant lymph nodes was the presence of pericapsular vessels.[78]

Interestingly, the normal characteristics of specifically medial iliac lymph nodes were described later. These normal lymph nodes exhibited a rapid inflow slope, in which a central artery was clearly visualized. Small intranodal vessels then radiated perpendicular to this central artery in a centrifugal fashion. The intranodal vessels were not able to be visualized with standard color or power Doppler prior to contrast administration. Finally, a diffuse, homogeneous enhancement period was noted throughout the lymph node followed by gradual decrease in contrast intensity.[79]

CEUS has also been used to trace lymphatic drainage of normal canine mammary tissue to identify sentinel lymph nodes. On average, it took 3 minutes for contrast to be visualized within the sentinel node after administering ultrasound contrast media directly into the mammary tissue. Core needle biopsy was then performed under CEUS guidance.[80]

When renal perfusion characteristics in dogs were first analyzed using CEUS, an important differentiation was made between the intensity of the cortex and the medulla. It was found that the cortical perfusion had a more rapid inflow and reached a higher peak intensity compared to the lower inflow and lower peak intensity seen in the medulla. This change is logical, as the cortex receives blood supply prior to the medulla, and that the microbubbles suffered some degree of destruction by the time they reached the medulla.[81]

Similar intensity changes were noted between the renal cortex and medulla when feline kidneys were analyzed. Again, a lower inflow slope resulted in a longer time to peak intensity for the medulla compared to the cortex. The cortex also exhibited a rapid enhancement pattern while the changes within the medulla appeared more gradual. At peak medullary enhancement there was a uniform hyperechoic appearance of the kidney resulting in loss of corticomedullary distinction. This study also evaluated contrast-enhanced power Doppler and noted an improvement in signal, particularly in historically low flow regions like the periphery of the cortex.[82]

When evaluating focal mass lesions in the kidney of dogs or cats, many pathologic conditions appear similar on standard B-mode ultrasound. A few neoplasms were able to be distinguished, however, based on their appearance after contrast administration. Renal carcinomas appeared to have large, tortuous arteries which exhibited earlier enhancement than the adjacent renal vessels. Hemangiosarcoma (only studied in the dog) appeared nonenhancing in both the early arterial and late corticomedullary phases. There were also additional lesions noted after contrast was added. The remaining pathologies, which included various other neoplasms as well as benign lesions, had similar characteristics.[83]

CEUS has also been used to evaluate renal changes after tissue core needle biopsy. In this study, a 14 gauge needle biopsy was used and CEUS was performed either 30 minutes after the procedure or both immediately after as well as 30 minutes after the procedure. Compared to standard B-mode ultrasound, more lesions were noted post-biopsy with CEUS. In the cases where CEUS was performed immediately after biopsy, the lesions appeared hyperechoic initially but were all hypoechoic by 30 minutes post-biopsy. As the lesions were monitored weekly throughout the study, all lesions exhibited a gradual decrease in size and margins became less distinct, while echogenicity gradually increased until returning to normal. Most lesions had resolved by 2 weeks post-biopsy and in all cases lesions resolved by 3 weeks post-biopsy. This established useful parameters for monitoring renal lesions after biopsy.[84]

Few studies have examined the utility of CEUS for characterizing certain adrenal gland disorders. One study examining the appearance of normal canine adrenal glands, observed rapid, homogeneous enhancement which began in the medulla and quickly involved the cortex. A gradual uniform washout period was noted. The optimal time for imaging acquisition, however, varied greatly between animals and ranged from 5-90 seconds post-injection.[85]

Bargellini et al compared normal dogs to those with diagnosed pituitary-dependent hyperadrenocorticism (PDH). The normal dogs again exhibited homogeneous contrast enhancement of the adrenal glands

which increased from the medulla to the cortex and gradually decreased in the washout phase, similar to the previously mentioned study.[85] For those dogs with PDH, there were 3 perfusion patterns noted, which all exhibited "rapid, chaotic" enhancement that occurred simultaneously within the medulla and the cortex. However, the perfusion pattern itself was not the only significant difference observed. Peak perfusion intensity, adrenal blood flow, and adrenal blood volume were all found to be greater in dogs with PDH. [86]

A single study has evaluated the utility of CEUS in distinguishing between malignant neoplasms of the pancreas in dogs. Although only a small study population, insulinomas appear hypervascular. To the contrary, adenocarcinomas appeared both hypoechoic and hypovascular.[87]

In contrast to human medicine, the cardiac applications of CEUS in veterinary medicine have been sparsely investigated to date. One study sought to determine the pulmonary transit time in normal cats. Using the right parasternal short axis echocardiogram view, the transit time between the pulmonary artery and the left atrium was recorded, averaging 4.12 +/- 1.0 seconds.[88]

B-mode ultrasound is a tool which aids in the diagnosis of retinal detachment and vitreous membranes; only recently has CEUS been evaluated for this purpose. In one study, CEUS was 100% accurate to help distinguish between the two disease processes. Persistent retinal perfusion was seen in patients with retinal detachment, even if partial, and was characteristic enough to differentiate from vitreous membranes.[89]

CEUS evaluation of the genital system is also limited and has involved strictly male canine reproductive organs to date. A study evaluating the utility of CEUS for characterizing blood flow of the normal canine prostate gland, only went so far as to improve categorizing the gland's blood flow from poor before contrast administration to moderate or good after contrast administration. Other than describing the

vascular pattern as "symmetric" and "diffuse", further characterization of the enhancement pattern was not achieved. The overall prostatic vascular area and vascularity index improved with contrast administration. Also, the use of power Doppler was found to be superior to color Doppler.[90]

Another study compared perfusion characteristics of normal canine testes to diseased testes, using histopathology for final diagnosis. The normal testes exhibited a homogeneous, rapid enhancement for both the wash-in and wash-out phases. The most common pathologic process observed in this study population was neoplasia, with interstitial cell tumors being most common. The most common non-neoplastic condition observed was testicular degeneration. Neoplastic conditions exhibited a heterogeneous, hyperenhancing pattern, with seminomas further characterized as having persistent enhancement of central vessels amongst a hypo- to isoechoic background. Non-neoplastic conditions had overall poor perfusion, classified as scant to moderate homogeneous enhancement.[91]

Research in the field of CEUS analysis of the gastrointestinal tract is lacking. The small intestine was evaluated in normal cats and there was individual wall layer distinction in the wash-in phase. The serosal and submucosal layers rapidly enhanced after contrast administration, followed by enhancement of the remaining wall layers so that by peak enhancement wall layers could not be distinguished. The wash-out phase was gradual, with the submucosal layer the last to linger.[92]

The second CEUS study involving the gastrointestinal tract was intra-operative. This study evaluated the enhancement characteristics of canine jejunum intra-operatively, and also sought to determine whether the transcutaneous doses previously used were adequate or whether dose adjustment needed to be made for the intra-operative approach. In this study, 9 dogs were evaluated intra-operatively after routine laparotomy approach was made and the abdomen was filled with saline to act as a contact medium. The transducer was then placed into a gel-filled sterile sleeve to be manipulated by the surgeon. Three doses of contrast agent were tested on each patient – 0.007ml/kg, 0.015ml/kg, and 0.03ml/kg. The resulting

images were analyzed and subjectively graded for arterial enhancement, jejunal mural enhancement, and homogeneity of mural enhancement. It was found that jejunal wall enhancement was homogeneous and occurred simultaneously between both the mesenteric and anti-mesenteric portions. Subjectively the 0.03ml/kg dose resulted in the most desirable images. Interestingly, peak intensity was found to be directly proportional to the contrast dose administered, while the outflow slope remained similar regardless of dose received.[11]

Acute intestinal ischemia in human medicine:

Overall, the incidence of acute bowel ischemia or infarction in human patients accounts for only 1% of cases presenting for acute abdominal signs[93] and 2% of gastrointestinal disease.[94] However, due to a variety of factors, including difficulty in obtaining an early and accurate diagnosis, the mortality rate remains markedly elevated and is estimated to be between 50-90%.[93,95,96] The downfall in using traditional abdominal radiography for this process is that the acute phase can go unrecognized. In fact, it has been reported than over 25% of cases will have completely normal abdominal radiographs.[97] Often only the later phases of the disease can have appreciable changes, with such radiographic signs including intestinal dilation, pneumatosis, or gas within the portal vein. Routine B-mode abdominal ultrasound is also difficult, as these patients are often severely painful and poorly compliant. Imaging can also be limited by a large amount of gas within the intestinal tract. Ultrasound can be useful, however, to evaluate for and rule-out other causes of acute abdominal signs including pancreatitis, cholecystitis,[93] or aortic aneurysm.[97] The best imaging route for identifying intestinal ischemia is selective mesenteric angiography,[93,97] which has a reported sensitivity of 87.5%-100%[96,97] and specificity of 100%.[97] However this modality is often not utilized due to unavailability of the procedure at certain institutions, high expense, and high invasiveness of the procedure.[93] Magnetic resonance imaging with angiography has also been utilized for evaluation of acute abdominal cases and is excellent for detecting occlusive and

thromboembolic diseases of the celiac trunk, superior mesenteric artery, portal vein, and mesenteric veins. In fact, in cases of portal or mesenteric thrombosis, the sensitivity, specificity, and accuracy are reported to be 100%, 98%, and 99% respectively. However, magnetic resonance angiography has limited usefulness for diagnosis of peripheral occlusive disease or non-occlusive disease.[97] Computed tomography is currently the imaging modality of choice for cases of suspected intestinal ischemia, with a specificity of 92-100% and sensitivity of 64-96%.[93,95,97,98] This procedure also has the added benefits of being non-invasive, rapidly performed, providing excellent spatial resolution, the ability to perform 2D or 3D reconstructions, and the added utility of angiography.[93]

A variety of laboratory parameters have also been evaluated in patients with mesenteric ischemia. However, most parameters, including D-lactate, L-lactate, D-dimer, and alpha-glutathione S-transferase (GST) levels, have all resulted in highly variable and non-specific results.[98] One laboratory parameter under investigation which has shown promising results is intestinal fatty acid binding protein (IFABP). This protein is located within the mucosal layer of small intestine and is involved with fatty acid transport and storage. In cases of intestinal injury, IFABP is hypothesized to translocate to systemic circulation and the substance can be measured in urine. Preliminary results show IFABP to be a reliable marker for small intestinal injury resulting from ischemia, but work remains to be completed to establish its clinical utility[99] as variations in its levels have only been shown after transmural bowel infarction has developed. Therefore its usefulness in diagnosing earlier stages of the disease might be limited.[97]

It is important to differentiate acute mesenteric ischemia from chronic mesenteric ischemia or ischemic colitis, as the treatment of choice for acute mesenteric ischemia is immediate surgical intervention. Chronic mesenteric ischemia occurs due to gradual stenosis of the arterial supply to the intestinal tract, usually secondary to atherosclerosis. Patient presenting with abdominal pain can be differentiated from acute cases, as chronic mesenteric ischemia tends to result a complaint of post-prandial pain. Patients will also suffer from recurrent pain episodes and chronic weight loss. Acute mortality is not associated with

this disease. Colonic ischemia again is also associated with atherosclerosis, but of the colonic arterial supply. The result is colonic ischemia secondary to hypotension or vascular spasm.[98]

The small and large intestines are supplied by three arteries: the celiac trunk, the superior mesenteric artery, and the inferior mesenteric artery.[96] The venous system runs in parallel to the arterial system, and includes the superior mesenteric vein, inferior mesenteric vein and their lesser branches.[97] Normally, 20% of resting cardiac output is dedicated to the intestinal tract. Of this, approximately 2/3 supplies the intestinal mucosa. This percentage of cardiac output may increase up to 35% during post-prandial periods and decrease as low as 10% in critical stress situations. Both local myogenic and systemic autoregulation of the vascular supply occur.[96] The small intestine can tolerate up to a 75% reduction is blood flow for up to 12 hours before irreversible damage occurs.[98]

The majority of human cases of acute intestinal ischemia are comprised of occlusive and thromboembolic diseases while non-occlusive diseases make up a smaller portion, as the former two categories total approximately 80% of cases and the latter only approximately 20%. Occlusive causes are mostly caused by intestinal volvulus, however intestinal torsion, bowel occlusion, or bowel over-distension are also possible.[93] The volvulus is referred to as a closed-loop obstruction, which is caused by an adhesive band or hernia and involves the mesentery and mesenteric vasculature. After the initial volvulus, venous outflow is impaired and arterial ischemia follows. Congestion and hemorrhage occur within the bowel wall and mesentery, and intestinal dilation and fluid distension are often noted. In cases of closed-loop obstruction, the intestines appear as a “C” or “U” shape and the mesentery forms a fan-shape, with the mesenteric vessels converging at the site of obstruction.[95] The majority of cases of intestinal thromboembolic causes are split equally between superior mesenteric artery embolization and arterial thrombosis.[93] The superior mesenteric artery is the most common artery affected by embolism, attributed to its larger diameter and angle of origin from the aorta. The majority of these emboli lodge distally within the superior mesenteric artery as its diameter begins to taper, usually past the origin of the middle

colic artery.[97] Small intestinal thromboembolic cases can be a result of cardiac disease such as endocarditis or atrial fibrillation, atherosclerosis, arterial dissection, spontaneous or post-operative cholesterol embolization, surgery, or stent placement.[96] Venous thrombosis occurs rarely and accounts for only 10-15% of thromboembolic cases.[93] Thrombosis is twenty times more likely to affect the superior mesenteric vein than the inferior mesenteric vein, due to its larger diameter and flow characteristics. Causes of venous thrombosis include hypercoagulable syndromes, portal hypertension, abdominal infection, and trauma.[97] Non-occlusive disease is caused by a severe reduction in blood flow, while the arteries and veins remain patent.[93] Vasopressin and angiotensin are suspected to play a role in mediating vasoconstriction via the sympathetic nervous system.[97] Causes are many and include such conditions as hypovolemia, hypotension, and heart failure.[93,97]

Intestinal ischemia occurs in three phases, which vary in prognosis and treatment. The first is acute mesenteric ischemia. This phase results in vascular alterations, can last up to 12 hours, and can be reversed if diagnosed early in its course.[93] Effects are only to the mucosal layer of the bowel and include ulceration, erosion, hemorrhage, or superficial necrosis. This initial phase also can cause the release of inflammatory mediators such as cytokines, platelet-activating factor, and tumor necrosis factor. These substances can contribute to the pathogenesis of bowel necrosis as they cause additional damage to the bowel wall through disruption of the mucosal barrier. The second phase of bowel ischemia is partial mural bowel ischemia. Changes are similar to the first phase, but effects extend deeper into the bowel wall and changes are noted in both the submucosal and muscular layers. Fibrous tissue may develop at the site of injury and stricture may form if the patient recovers.[96] The third phase of bowel ischemia is mesenteric infarction. This phase results in transmural bowel necrosis and is the phase which definitively requires immediate surgical intervention, as the intestinal changes are not reversible and are life-threatening.[93] Sequelae to transmural bowel necrosis may also include intestinal bleeding, intestinal perforation, abscess formation, and peritonitis. Systemic effects may include myelosuppression, myocardial failure, renal failure, and disseminated intravascular coagulation.[96]

Complete abdominal CT consists of both pre- and post-contrast scans of the entire abdomen. Both oral and rectal administration of water or contrast material is recommended prior to the CT procedure in order to better distend the bowel lumen for evaluation of the bowel wall. Either positive or negative contrast agents can be used for this purpose. Pre-contrast, known as "unenhanced", images can be evaluated for calcifications or hyperattenuating clots within the vascular system. Comparison between the pre- and post-contrast images is necessary to differentiate causes of a hyperattenuating bowel wall, including intramural hemorrhage, hyperemia, or hyperperfusion. Angiography is achieved by administering a non-ionic iodinated contrast agent intravenously at a rate of 100-150ml total volume using a power injector at 2-4ml/sec. With multi-detector CT, biphasic angiography technique is used to acquire images in both the arterial and venous phases. The arterial phase is approximately 25-30 seconds after the start of contrast injection and portal venous phase is approximately 60 seconds after the start of contrast injection. If single detector CT is being used, a single post-contrast portal venous phase is obtained. Sagittal, coronal, and curved multiplanar reformatted images and CT angiograms can then be created using post-processing software.[96]

In cases of acute mesenteric ischemia, changes observed on CT angiography begin with vasodilation. This manifests as persistent hyperattenuation of the bowel wall through both the arterial and venous post-contrast phases. The vasoconstrictive phase follows vasodilation. This appears as persistent hypo- or non-contrast enhancing bowel wall. The third phase is increased capillary permeability which causes intestinal edema, hemorrhage, and inflammatory infiltrates. CT images will reveal bowel wall thickening and intestinal dilation.[93] Bowel wall thickening is reported to be the most common CT finding in acute bowel ischemia, and found to be present in 26-96% of cases.[96] Normal bowel wall should measure between 3-5mm and in cases of altered perfusion is expected to increase to 8-9mm.[95] Bowel wall thickness is however significantly affected by the degree of intestinal distention.[96] Mucosal cellular necrosis will follow and be seen as pneumatosis or gas within either the portal vein or mesenteric vein branches. Finally, transmural bowel necrosis occurs and pneumoperitoneum or ascites will be noted.[93]

Edema within the mesenteric fat, known as fat-stranding, may also be noted in these advanced cases.[95] Specificity for partial mural or transmural bowel ischemia is as high as 94% if mesenteric fat-stranding is seen in conjunction with either mesenteric fluid or ascites.[96] The site of vascular occlusion, whether from occlusive or thromboembolic disease, can be better visualized if the site is at a main vascular trunk and is accurately diagnosed on CT angiography in 58% of cases.[93]

A common area where CT findings can be misinterpreted includes mistaking intestinal spasticity for a normal peristaltic contraction. Spastic contractions can be seen particularly in cases where ischemic injury is confined to the mucosal layer. One way to avoid such misinterpretation is to distend the bowel lumen with oral or rectal contrast agents as described previously. Another common pitfall is to interpret a segment of thickened intestinal wall as normal if its wall thickness still falls within the 3-5mm wall thickness range. For example, a segment which has increased wall thickness but is also significantly distended may still fall in the normal wall thickness range. The final common mistake is to interpret dilated intestine as a functional ileus or pseudo-obstruction. This may happen in very acute cases, where concurrent intestinal wall thickening has not had time to occur.[96]

Recent Advances in Imaging the Canine Abdomen:

Traditional imaging techniques of the abdomen are comprised of survey radiographs or abdominal ultrasound. Radiographic and ultrasonographic evaluation criteria of surgical small intestinal diseases, such as mechanical intestinal obstruction, are well-defined. Common radiographic signs of mechanical intestinal obstruction include segmental intestinal dilation, abnormal intestinal location, intestinal plication, or the visualization of an ingested foreign object or mass itself. The radiographic cut-off recommended for defining dilated small intestine in the dog is 1.6 times the height of the fifth lumbar vertebral body.[100] A newer study suggests not only evaluating the fifth lumbar vertebral ratio, but also the

ratio of largest to smallest small intestinal diameter and the ratio of largest to average small intestinal diameter to improve accuracy of mechanical obstruction diagnosis based on radiographs alone.[101] A large pitfall of radiographic evaluation of the gastrointestinal tract is due to superimposition of intestinal loops and their contents.[102] Sonographic signs of mechanical small intestinal obstruction again include intestinal dilation, but findings also commonly noted are increased bowel wall thickness or abnormal intestinal motility.[103] When directly comparing the two imaging modalities, however, ultrasound has been shown to be superior for reaching a definitive diagnosis of small intestinal mechanical obstruction more accurately. In one recent study a definitive result was predicted in 70% of patients based on radiography compared to 97% of patients based on ultrasound.[104] Limitations of ultrasound for evaluation of the gastrointestinal tract are also present, and most notably include the inability to visualize intestinal structures or wall character deep to bowel gas.[102]

CT is rapidly becoming the preferred imaging route for canine patients presenting with abdominal disease, largely due to the optimization of imaging protocols that no longer require the use of general anesthesia. In a recent study, eighteen dogs were prospectively enrolled after presenting for acute abdominal signs. Dual-phase angiography was performed after survey CT was completed, in order to specifically evaluate both the arterial and portal venous phases. Eight patients were able to be scanned awake while ten were minimally sedated. Sedation protocols were chosen at the discretion of the attending veterinarians and most often were comprised of an opiate with or without a benzodiazepine. Half the patients were scanned using a positioning device called the VetMouseTrap™ (University of Illinois, Urbana, IL) while the remaining patients were positioned in a standard foam trough.[105] The VetMouseTrap™ is a positioning device which allows for awake patient imaging, requires no patient manipulation or restraint, and was originally tested for use in cats.[106,107] Median scan time was approximately eight minutes. Only two patients were judged to have poor scan quality, due to motion artifact or beam hardening from previous barium administration respectively. The remaining scans were

qualified as excellent (9), good (4), or fair (3). No dogs exhibited complications during the procedure, making this a safe and rapid test for patients with abdominal signs.[105]

Another study investigated a variety of protocols to optimize the use of awake or sedated CT scans as a primary screening tool for patients with suspected abdominal disease. They utilized a 16-detector row helical CT scanner, varying pitch and milliamperage (mA) for each scan, while kVp remained constant at 120. Images were acquired using a CT phantom, canine cadaver, and 27 prospectively recruited canine patients. They found the protocol using a pitch of 1.25 and mA of 60 was the most optimal. Although more streak artifact was noted in the smaller weight group (<10 kg) and more motion artifact and quantum mottle was noted in the larger weight group (>25 kg), there was no significant difference in overall artifact scores between protocols and in no case did the artifact render the scan non-diagnostic.[108]

As for CT evaluation of the gastrointestinal tract specifically, literature is still lacking in the veterinary field. In a recent retrospective study, abdominal CT images of 19 canine patients were reviewed for analysis of the gastrointestinal tract. These patients underwent imaging for reasons unrelated to gastrointestinal disease. Overall CT obtained small intestinal diameter was compared to the height of the fifth lumbar vertebrae and colon diameter was compared to the length of the seventh lumbar vertebrae, as traditional radiographic measurements would be performed. CT measured intestinal wall thickness was compared to historical normal ultrasonographic wall measurement parameters. Overall CT-obtained measurements correlated well with the historical radiographic and ultrasonographic measurements.[102]

This same study also retrospectively evaluated two canines with known gastrointestinal disease. One patient had a small gastric leiomyosarcoma. The second patient had focal jejunal disease consistent with adenocarcinoma and concurrent lymphoplasmacytic enteritis. In both cases the CT measured wall thickness at the lesion site was above the ultrasound normal range and in the latter, the overall intestinal diameter was also increased compared to the radiographic standard.[102]

A study analyzing the direct comparison between ultrasound and CT for the detection of abdominal lesions was first published in 2012. Twenty-seven dogs were prospectively recruited for abdominal ultrasound and minimally sedated contrast-enhanced abdominal CT. For patients in the smaller weight classes (<25 kg), there was no difference in number of clinically significant lesions detected between imaging modalities. However in patient in the larger weight class (>25 kg), CT detected more clinically relevant lesions and also detected a larger quantity of lesions overall. Due to this discrepancy in the larger patients, there was a poor agreement between CT and ultrasound for lesion detection, with only 23% agreement seen in patients weighing larger than twenty-five kilograms. In all cases, yet again, no adverse reactions were noted with the administration of CT contrast nor were any CT motion artifacts significant enough to affect interpretation.[109]

There are limited studies investigating the utility of magnetic resonance imaging (MRI) for evaluating the canine abdomen. The higher overall cost, required use of general anesthesia, and equipment availability are considered general limiting factors of MRI. One recent study, however, helped better define an optimal scanning protocol if a patient should require this form of abdominal imaging. Three sequences were found to be ideal for evaluating the canine abdomen, including dorsal T2 turbo spin echo (TSE) with fat saturation and breath-hold technique, transverse T1 turbo fast low-angle shot gradient echo (FLASH GRE) with breath-hold technique, and dorsal T2 half-Fourier acquisition single-shot turbo spin echo (HASTE) with respiratory navigation. Overall these three sequences were found to have short acquisition times, had similar diagnostic quality, and yielded complementary information.[110]

Research comparing multiple imaging modalities with the use of CEUS for the analysis of abdominal disease is extremely lacking. One recent study, however, aimed to do just that. Nineteen dogs presenting with acute abdominal signs were prospectively enrolled. In this study, survey abdominal radiographs, standard B-mode ultrasound, contrast-enhanced ultrasound, and multiphase contrast-enhanced CT was performed and modalities were compared in their ability to determine surgical from non-surgical disease.

Interestingly, all dogs had the CT performed while they were either awake or minimally sedated. CEUS was performed focally at the suspected clinically relevant lesion site.[111]

Eight patients were determined to have non-surgical disease, with ailments such as pancreatitis or gastric lymphoma determined to be the clinically relevant lesion. The remaining eleven patients with surgical disease had hepatic abscess, splenic abscess, gastric lymphoma with perforation, small intestinal mechanical obstruction, or traumatic diaphragmatic hernia of the spleen. The small intestinal mechanical obstruction cases were further characterized as linear foreign bodies (4), focal proximal jejunal obstruction secondary to a corn cob (1), and combined gastric and jejunal obstructive cloth material (1). In the two cases of hepatic abscessation, imaging findings alone were considered insufficient to determine whether the case was surgical, and instead cytological diagnosis was necessary. This left a total of nine cases in which imaging findings were considered sufficient to determine surgical disease.[111]

Both radiographs and ultrasound identified the majority of cases (8/9) as surgical, while CT identified all potential cases as surgical (9/9). Although most imaging modalities demonstrated at least moderate agreement, there was poor agreement in detecting pneumoperitoneum and determining pancreatic lesion size between routine and contrast-enhanced ultrasound. Pneumoperitoneum was actually not detected on ultrasound in either of the two affected cases. Both the overall size and number of lesions were also frequently underestimated on both ultrasound modalities compared to CT. In over half of the cases (11/19), the routine ultrasound exams were considered incomplete, mostly as they were lacking small parts such as the identification of adrenal glands or lymph nodes.[111]

However, when analyzing the presence of perfusion deficits, CT often failed to detect perfusion deficits that were seen on CEUS. Perfusion deficits were present on CEUS in the cases of gastric lymphoma (2/2), small intestinal mechanical obstruction (2/6), pancreatitis (7/7), and hepatic abscess (2/2). Comparatively, perfusion deficits were present on CT in cases of pancreatitis (3/7) and hepatic abscess

(1/2). Hypotheses proposed by the group as to the stark difference in perfusion deficit detection between modalities was the excellent sensitivity of contrast ultrasound microbubbles as well as the improved spatial and temporal resolution of ultrasound compared to CT allowing CEUS to detect smaller lesions. In both cases in which perfusion deficits were detected in small intestine, surgery ultimately required jejunal resection and anastomosis. Patient outcome of these two cases was ultimately poor, as both died. One death was during hospitalization and the other was shortly after the patient was discharged. Due to favorable results with both CT and CEUS, the authors recommended performing CT followed by focused CEUS at the site of the abdominal lesion to obtain the most accurate results. The clinical relevance of the small intestinal perfusion deficits found in this study, however, remain unknown. An interesting trend was noted, but further investigation is warranted, particularly comparing the pre-operative imaging findings with intra-operative findings, histopathology, and patient outcome.

CHAPTER 2

COMPARATIVE IMAGING OF SURGICAL SMALL INTESTINAL DISEASE IN DOGS: EVALUATION OF PRE-OPERATIVE CONTRAST-ENHANCED ULTRASOUND, INTRA-OPERATIVE CONTRAST-ENHANCED ULTRASOUND, AND TRIPLE-PHASE CONTRAST-ENHANCED COMPUTED TOMOGRAPHY

Introduction:

Small intestinal diseases requiring surgery are a common occurrence in veterinary practice, with the ingestion of obstructive foreign material being a frequent cause.[112–115] Other causes of obstruction of the gastrointestinal tract include intussusception, neoplasia, adhesions, or stricture.[112] If blood supply to the intestine is comprised, intestinal wall necrosis can follow and subsequent intestinal resection be required. Failure to identify ischemic tissue can increase the risk of intestinal anastomotic leakage.[115] Dehiscence of either enterotomy or intestinal resection and anastomosis sites may lead to generalized bacterial peritonitis and subsequent death.[115] Perfusion studies performed with ultrasound contrast media could aid in non-invasive prediction of tissue viability and functionality.[4]

Recent studies have compared contrast-enhanced computed tomography (CT) to routine B-mode ultrasound for evaluation of the canine abdomen[102,109,111] but limited information has been obtained evaluating the use of contrast-enhanced ultrasound for interrogation of the gastrointestinal tract.[11,111] One recent study found that contrast-enhanced ultrasound (CEUS) was able to identify perfusion deficits within the pancreas and gastrointestinal tract that were not detected on contrast-enhanced computed tomography.[111]

The objectives of this study were threefold: 1) to compare contrast-enhanced computed tomography, pre-operative contrast-enhanced ultrasound, and intra-operative contrast-enhanced ultrasound to determine which imaging modality best detects perfusion deficits within the small intestine of dogs, 2) to evaluate whether any imaging findings correlate with the presence of a perfusion deficit, and 3) to determine

whether there is an association between specific imaging findings and patient outcome. Our hypotheses were that 1) intra-operative contrast-enhanced ultrasound would best detect ischemic lesions within the gastrointestinal tract, 2) no specific imaging finding(s) would be consistently associated with the presence of ischemia, and 3) the presence of a perfusion deficit on any imaging modality would be associated with poor patient outcome.

Materials and methods:

All protocols were approved by the Institutional Animal Care and Use Committee of the University of Illinois. Client-owned dogs that presented to the University of Illinois Veterinary Teaching Hospital between January 2014 and August 2014 were prospectively recruited following owner consent. Recruitment criteria included a surgical gastrointestinal condition diagnosed by B-mode abdominal ultrasound. The ultrasound exam was performed by a board-certified radiology faculty member or radiology resident on duty at the time of patient admission. Qualifying gastrointestinal disorders were to involve or have a high clinical suspicion for involvement of the small intestine, and were to have the potential for small intestinal resection.

Routine B-mode ultrasound was followed immediately by a focused CEUS (MyLab70XVG, Esaote, Indianapolis, IN) at the site of the intestinal lesion or, if a larger area of intestine was affected than could be interrogated within the field of view, at whichever intestinal site was subjectively deemed most severely affected. A linear array transducer (3-11 MHz) was used**.** Ultrasound settings, including depth of field, time gain compensation, and overall gain, were adjusted at the user's discretion. The focal zone was set at or just below the area of interest. Power was set at 5% and mechanical index at 0.03. All CEUS exams were performed by the same radiology resident (EP). The microbubble contrast agent (Definity^{TM}, Lantheus Medical Imaging, North Billerica, MA) was prepared by a commercial agitator

(Vialmix, North Billerica, MA) prior to use according to manufacturer instructions. A rapid bolus injection of microbubble contrast agent was then administered directly into an indwelling cephalic venous catheter using a 1ml syringe and 22G 1.5" needle. Bolus contrast injection was followed by 5ml saline flush using a 6ml syringe and 22G 1" needle. For patients weighing less than 20kg, 0.1ml microbubble contrast agent was used per injection. For patient weighing greater than 20kg, 0.2ml microbubble contrast agent was used according to previously published doses.[69,116] An image series clip was recorded at 25 frames per second for 120 seconds beginning immediately after the start of contrast injection. Each patient received 1-2 total contrast injections. For those patients requiring multiple injections, the bubbles were destroyed by temporarily raising the mechanical index, waiting for 5 minutes between injections, or a combination of both until tissues appeared to return to background intensity.

Following CEUS, all patients underwent survey and triple phase contrast-enhanced abdominal CT using a 16-slice helical CT scanner (GE Lightspeed 16 slice CT, Milwaukee, WI). Patients were positioned in dorsal recumbency and given light sedatives if necessary to avoid patient movement. Anesthetic agents used were at the discretion of the attending clinician. CT parameters were adjusted accordingly per patient and were as follows: kV of 120, mA of 180-300, slice width of 2.5mm with 1.25mm overlap, 25-50cm scan field of view, 512 x 512 matrix, 0.938:1 to 1.375:1 collimator pitch, and 0.5s rotation time according to previously published protocols.[105] Multiplanar image reconstruction was performed in dorsal and sagittal planes with a slice width of 0.625mm. Pre-contrast abdominal CT was followed by triple-phase post-contrast image acquisition. Post-contrast scan delays of 20 seconds, 40 seconds, and 120 seconds after the start of contrast injection were used to obtain arterial, portal venous, and delayed vascular phases.[105,117,118] A dose of 2ml/kg (600 mg I/kg) non-ionic iodinated contrast (Omnipaque-300™ Iohexol injection, GE Healthcare, Princeton, NJ) was administered intravenously through a peripheral venous catheter, with a maximum dose of 60ml per patient. For patients receiving less than 20ml, contrast was administered by rapid hand-injection bolus. For patients receiving greater than 20ml,

contrast was administered by power-injector (Medrad Vistron CT Injection System, Indianola, PA) at a rate of 2-3ml/sec followed by a 10ml saline flush.[105]

Immediately following imaging, all patients were placed under general anesthesia for routine ventral midline laparotomy. Upon entrance into the abdomen, the gastrointestinal lesion was isolated and packed off using moistened laparotomy sponges. Ultrasound gel was placed into the end of a sterile palpation sleeve. The sleeve was then placed over the ultrasound probe in sterile fashion by the surgeon. The covered transducer was then placed directly and gently on the intestinal lesion by the surgeon with the intestinal segment in longitudinal axis to the transducer. The surgeon performing the CEUS exam varied as to the surgical resident or faculty member on-duty. If adequate ultrasound probe contact could be maintained directly on the lesion, a focused CEUS exam was performed at that time prior to any surgical intervention at the lesion site. In several cases of discrete intestinal obstruction this was not possible due to the contour of the lesion, in which case the CEUS was performed at the surgical site once the luminal material was removed. If luminal foreign material was able to be manually manipulated retrograde into the stomach for surgical retrieval via gastrotomy, the CEUS was performed at the gastrotomy site. A single operator (EP) recorded the exam using the same imaging parameters and contrast injection protocol as the pre-operative CEUS. Between 1-3 contrast injections were performed per patient. Anesthetic parameters were closely monitored during and after contrast injection and no adverse reactions were noted.

Resected intestinal tissue was collected and fixed in formalin prior to routine tissue processing for histopathology. If surgical intestinal resection was not clinically indicated, a full-thickness biopsy from the surgical site was collected and submitted. Each case was reviewed by the pathology faculty or resident on-duty at the time in order to provide timely information to the clinicians providing treatment for each case.

Ultrasound data was downloaded for analysis offline. Image video clips were evaluated retrospectively by two reviewers (JM, EP) until consensus was reached as to the presence or absence of non-enhancing or hypoenhancing lesions. Images were then converted to tagged image file format (TIFF) sequences (Adobe After Effects, CC 2014, San Jose, CA). To correct for time, subsequent analysis was performed on the first of every 25 frames using image analysis software (ImageJ, National Institutes of Health, Bethesda, MD). A region of interest (ROI) was manually drawn to include the as much of the intestinal wall as possible at the site of interest and then manually adjusted as needed to account for any respiratory motion. The same ROI was continued throughout the image analysis for each image series. Pixel intensity of the ROI was recorded and used to generate a time-intensity curve (Excel, Microsoft, Redmond, WA) for each contrast injection administered. Perfusion parameters calculated included baseline, time to initial rise, inflow slope, time to peak, peak intensity, and outflow slope. Slopes were calculated using data points 20% above baseline and 20% below peak to exclude variability (Fig. 1).[11]

The primary transverse CT images were retrospectively reviewed by a single radiology resident (EP) on a dedicated DICOM workstation. Window width and level were adjusted at the reviewer's discretion. A circular region of interest was drawn in the intestinal wall at the site of the lesion or most affected intestine, immediately orad to the lesion, immediately aborad to the lesion, and at a site of normal intestine. An attempt was made to choose a similar lesion location as those suspected to have been examined in the contrast ultrasound exams. The region of interest was drawn as large as possible and made to include the entire wall thickness. Areas were chosen which appeared to have the least amount of motion or obliquity to minimize volume averaging. Five regions were chosen for measurement for each site and the average of these measurements was also recorded. This was repeated for the pre-contrast, arterial, portal venous, and delayed contrast phases. Attempts were made to use the same measurement sites for all phases. The presence or absence of certain factors was recorded including: plication, intestinal distension, peritoneal effusion, fat-stranding, and pneumoperitoneum. On post-contrast images, the presence or absence of non-perfusing or hypoperfusing intestinal lesions was also recorded.

A single pathologist (MW) retrospectively reviewed each case using routinely stained hematoxylin and eosin samples. The reviewer was not blinded to the previous pathology report obtained at the time of case submission. Intestinal necrosis was classified on a scale of 0-5 using a previously published modified human pathological scoring system (Fig. 2 and 3).[119] Samples were reviewed for the presence or absence of necrosis, thrombosis, edema, hemorrhage, ulceration, and inflammation. Biopsies obtained from two patients were excluded from histopathology analysis as the only tissues available for analysis were obtained from a gastric biopsy. Owners or referring veterinarians were contacted by phone no sooner than six months after patient discharge to inquire as to patient's survival status.

Statistical Analysis:

Statistical analysis was performed using commercially available software (Stata® 13.1, StataCorp, College Station, TX). Data was assessed for normality using a histogram comparison and the Shapiro-Wilk test. The variability between CT ROI individual measurements were analyzed using a multilevel repeated ANOVA after square root transformation. CT and CEUS data were compared to histopathology findings using Mann-Whitney U, Fisher's exact, and logistic regression. Survival analysis was performed using a log-rank test and cox regression analysis. A P-value ≤ 0.05 was considered statistically significant.

Results:

A total of thirteen dogs were prospectively recruited between January and August 2014. Age ranged from 1-13 years (mean 5.6 years), with 9 castrated males, 5 spayed females, and 1 intact female. Breeds represented included Labrador Retriever (2), Doberman Pinscher (2), Dachshund (2), Golden Retriever (1), Pit Bull Terrier (1), Weimaraner (1), Miniature Schnauzer (1), and mixed breed (3). Weight ranged

from 2.1-54.5 kg (mean 27.2 kg). Patient data is summarized in Table 1. Patients presented with discrete foreign bodies (6), linear foreign bodies (5) including 1 patient which had a concurrent intussusception, abscess (1), and neoplasia (1). The neoplastic lesion was identified histopathologically as a gastrointestinal stromal tumor originating from the cecum with invasion into the adjacent portions of ileum and colon. Four patients required intestinal resection and anastomosis (linear foreign body with intussusception, discrete foreign body, abscess, and neoplasia) of either the jejunum (3) or ileocolic junction (1). The majority of patients that did not require resection and anastomosis received a jejunal biopsy from the surgical site (7). Histopathology samples were obtained from the stomach (2) in patients that were able to have their foreign material manually manipulated from the small intestine into the stomach during surgery. Four patients experienced complications during the post-operative hospitalization period. One of these patients underwent acute cardiac arrest one hour post-operatively. One patient developed fever and abdominal incision drainage on day three of hospitalization. Cytology performed of the incisional drainage revealed intracellular bacteria. The patient was placed on oral antibiotics and responded well to therapy. One patient developed surgical site dehiscence on day three of hospitalization that required repeat resection and anastomosis. One patient developed septic abdominal effusion on day eight of hospitalization and was euthanized. Four patients were deceased on follow-up including the two patients who died during the post-operative hospitalization period and two patients which died later (107 and 158 days after admittance date) from unrelated medical issues. Hospitalization duration ranged from 2-9 days, with a mean of 3.9 days including all patients enrolled and a mean of 3.2 days including only patients that survived to discharge.

First, the individual CT ROI measurements were analyzed for variability to determine whether the average could be used in our statistical analysis. As expected, there was a statistically significant difference between CT ROI measurements between phases ($p<0.001$) and between sites in each phase ($p=0.016$). However, between sites overall, the CT measurements were not significantly different

(p=0.215) indicating the measurements were similar. Therefore, only the average of the five CT ROI measurements for each site in each phase were used for all further data analysis.

Histopathology findings are summarized in Table 2. The chance of necrosis (p=0.003) and thrombosis (p=0.024) significantly increased with increased histopathology ischemia grade, however the presence of edema (p=0.576), hemorrhage (p=0.545), ulceration/erosion (p=0.061), and inflammation (p=0.061) had no significant association with ischemia grade.

Next, the CT data and histopathology findings were compared (Fig. 4). There was a statistically significant association between the subjective presence of a perfusion deficit on CT and both increased histopathology ischemia grade (p=0.048) and greater chance of necrosis (p=0.024). A perfusion deficit was visually detected in 3/4 (75%) of patients requiring a resection. No significant difference was found comparing the subjective presence of a perfusion deficit on CT and histopathology presence of thrombosis (p=0.152), edema (p=1.000), hemorrhage (p=0.182), ulceration/erosion (p=0.182), and inflammation (p=0.182).

The presence of intestinal plication observed on CT was not significantly associated with the histopathology presence of necrosis (p=1.000), thrombosis (p=1.000), edema (p=1.000), hemorrhage (p=0.545), ulceration/erosion (p=1.000), or inflammation (p=0.545). The presence of intestinal distension observed on CT was not significantly associated with the histopathology presence of necrosis (p=1.000), thrombosis (p=0.491), edema (p=1.000), hemorrhage (p=1.000), ulceration/erosion (p=1.000), or inflammation (p=1.000). The presence of peritoneal effusion observed on CT was not significantly associated with the histopathology presence of necrosis (p=0.491), thrombosis (p=1.000), edema (p=1.000), hemorrhage (p=0.182), ulceration/erosion (p=0.182), or inflammation (p=0.182). The presence of pneumoperitoneum observed on CT was not significantly associated with the histopathology presence of necrosis (p=0.109), thrombosis (0.491), edema (p=1.000), hemorrhage (p=0.455),

ulceration/erosion (p=0.455), or inflammation (p=0.455). The presence of fat-stranding observed on CT was not significantly associated with the histopathology presence of necrosis (p=0.088), thrombosis (p=0.491), edema (p=0.576), hemorrhage (p=0.545), ulceration/erosion (p=0.545), or inflammation (p=0.545). The histopathology ischemia grade was not significantly associated with the presence of intestinal plication (p=0.738), intestinal distension (p=0.77), peritoneal effusion (p=0.171), pneumoperitoneum (p=0.164), or fat-stranding (p=0.137).

There was no significant association between histopathology ischemia grade and the CT ROI measurements in the pre-contrast series at the lesion site (p=0.351), orad to the lesion (p=0.645), and normal intestine (p=0.868). However, a significant association was found, indicating increased histopathology ischemia grade correlated with lower HU values in the pre-contrast series aborad to the lesion (p=0.049). No significant association between histopathology ischemia grade and the CT ROI measurements in the arterial post-contrast series were found at the lesion site (p=0.497), orad to the lesion (p=0.056), aborad to the lesion (p=0.297), and in normal intestine (p=0.080). In the portal venous post-contrast CT series, no significant association was found between the histopathology ischemia grade and the ROI measurements at the lesion site (p=0.814), orad to the lesion (p=0.056), aborad to the lesion (p=0.264), and normal intestine (p=0.933). There was no significant association between the histopathology ischemia grade and the CT ROI measurements in the delayed post-contrast series at the lesion site (p=0.681), orad to the lesion (p=0.370), aborad to the lesion (p=0.623), and normal intestine (p=0.289).

There was no significant association between the presence of necrosis on histopathology and the CT ROI measurements in the pre-contrast series at the site of the lesion (p=1.000), orad to the lesion (p=1.000), aborad to the lesion (p=0.059), and normal intestine (p=0.57). There was no significant association in the arterial phase at the site of the lesion (p=0.57), orad to the lesion (p=0.086), or aborad to the lesion (p=0.732), however there was a significant association at normal intestine (p=0.017) which indicated

higher HU values were associated with a greater chance of necrosis. In the venous phase, there was no significant association at the site of the lesion (p=0.706), aborad to the lesion (p=0.706), or at normal intestine (p=0.45), however there was a significant association orad to the lesion (p=0.014) indicating higher HU values were associated with a greater chance of necrosis. In the delayed phase, there was no significant association at the site of the lesion (p=0.45), orad to the lesion (p=0.257), aborad to the lesion (p=0.85), or at the site of the lesion (p=0.257).

Regarding the presence of thrombosis on histopathology, there was no significant association in the CT ROI measurements in the pre-contrast series at the site of the lesion (p=0.683), orad to the lesion (p=0.838), or at normal intestine (p=0.152), however there was a significant association aborad to the lesion (p=0.025) indicating lower HU values were associated with a greater chance of thrombosis. For the arterial phase, there was no significant association at the site of the lesion (p=0.602), orad to the lesion (p=0.116), or aborad to the lesion (p=1.000), however there was a significant association at normal intestine (p=0.037) which indicated higher HU values were associated with a greater chance of thrombosis. In the venous phase, there was no significant association at the site of the lesion (p=0.838), aborad to the lesion (p=0.414), or at normal intestine (p=0.153), however there was a significant association orad to the lesion (p=0.041) which indicated higher HU values were associated with a greater chance of thrombosis. In the delayed phase, there was no significant association at the site of the lesion (p=0.54), orad to the lesion (p=0.307), aborad to the lesion (p=0.838), or at normal intestine (p=0.54).

For edema seen on histopathology, there was no significant association in the CT ROI measurements for the pre-contrast series at the site of the lesion (p=1.000), orad to the lesion (p=0.257), aborad to the lesion (p=0.706), or at normal intestine (p=0.776). In the arterial phase, there was no significant association at the site of the lesion (p=0.087), orad to the lesion (p=0.424), or at normal intestine (p=0.569), however there was a significant association aborad to the lesion (p=0.03) indicating lower HU values were associated with an increased chance of edema. In the venous phase, there was no significant association

at the site of the lesion (p=0.85), orad to the lesion (p=0.85), or aborad to the lesion (p=0.706), however there was a significant association at normal intestine (p=0.038) indicating higher HU values were associated with an increased chance of edema. In the delayed phase, there was no significant association at the site of the lesion (p=0.706), orad to the lesion (p=0.85), aborad to the lesion (p=0.45), or at normal intestine (p=0.85).

For hemorrhage seen on histopathology, there was no significant association in the CT ROI measurements for the pre-contrast series at the site of the lesion (p=0.1), orad to the lesion (p=0.584), aborad to the lesion (p=0.144), or at normal intestine (p=0.2). In the arterial phase, there was no significant association at the site of the lesion (p=0.831), orad to the lesion (p=0.134), aborad to the lesion (p=0.394), or at normal intestine (p=0.201). In the venous phase, there was no significant association at the site of the lesion (p=0.715), orad to the lesion (p=0.2), aborad to the lesion (p=0.465), or at normal intestine (p=0.465). In the delayed phase, there was no significant association at the site of the lesion (p=0.584), orad to the lesion (p=0.855), aborad to the lesion (p=0.465), or at normal intestine (p=0.273).

For ulceration or erosion seen on histopathology, there was no significant association between the CT ROI measurements in the pre-contrast series at the site of the lesion (p=0.584), orad to the lesion (p=0.715), aborad to the lesion (p=0.1), or at normal intestine (p=0.272). In the arterial phase, there was no significant association at the site of the lesion (p=0.347), aborad to the lesion (p=0.175), or at normal intestine (p=0.117), however there was a significant association orad to the lesion (p=0.028) indicating higher HU values were associated with an increased chance of ulceration or erosion. In the venous phase, there was no significant association at the site of the lesion (p=0.855), aborad to the lesion (p=0.855), or at normal intestine (p=0.855), however there was a significant association orad to the lesion (p=0.044) indicating higher HU values were associated with an increased chance of ulceration or erosion. In the delayed phase, there was no significant association at the site of the lesion (p=0.855), orad to the lesion (p=0.584), aborad to the lesion (p=0.361), or at normal intestine (p=0.201).

For the presence of inflammation on histopathology, there was no significant association between the CT ROI measurements in the pre-contrast series at the site of the lesion (p=1.000), orad to the lesion (p=0.144), aborad to the lesion (p=0.584), or at normal intestine (p=0.41). In the arterial phase, there was no significant association at the site of the lesion (p=0.917), orad to the lesion (p=0.463), aborad to the lesion (p=0.917), or at normal intestine (p=0.465). In the venous phase, there was no significant association at the site of the lesion (p=0.361), orad to the lesion (p=0.464), aborad to the lesion (p=0.855), or at normal intestine (p=0.361). In the delayed phase, there was no significant association at the site of the lesion (p=0.465), orad to the lesion (p=0.855), aborad to the lesion (p=1.000), or at normal intestine (p=0.361).

The associations between CEUS findings and histopathology were then analyzed (Fig. 5). There was no significant statistical association between histopathology grade and whether there was the subjective presence of a perfusion deficit on contrast ultrasound (p=0.995), however observers were able to visually detect perfusion deficits in 4/4 (100%) of patients requiring a resection. When comparing the pre-operative ultrasound ROI measurements and histopathology findings, there was no significant association between the histopathology grade and ultrasound baseline (p=0.079), time to initial rise (p=0.586), inflow (p=0.128), time to peak (p=0.204), peak (p=0.176), or outflow (p=0.426). Non-significant values were also found comparing histopathology grade to the intra-operative ultrasound baseline (p=0.058), time to initial rise (p=0.507), inflow (p=0.132), time to peak (p=0.182), peak (p=0.126), or outflow (p=0.407).

The presence of inflammation on histopathology was compared to the pre-operative ultrasound measurements and found no significant association with ultrasound baseline (p=0.197), time to initial rise (p=0.23), inflow (p=0.465), time to peak (p=0.271), peak (p=0.273), or outflow (p=1.000). No significant association was found with intra-operative ultrasound baseline (p=0.783), time to initial rise (p=0.784), inflow (p=0.584), time to peak (p=0.359), peak (p=0.715), or outflow (p=0.409).

The presence of ulceration or erosion on histopathology was compared to the pre-operative ultrasound measurements and found no significant association with ultrasound baseline (p=0.097), time to initial rise (p=0.782), inflow (p=0.715), time to peak (p=0.521), peak (p=0.715), or outflow (p=0.855). No significant association was found with intra-operative ultrasound baseline (p=0.169), time to initial rise (p=0.647), time to peak (p=0.271), peak (p=0.715), or outflow (p=0.927). However, there was a significant difference associated with the presence of ulceration or erosion and the intra-operative ultrasound inflow slope (p=0.045) indicating a greater inflow slope was associated with an increased chance of ulceration or erosion.

The presence of hemorrhage on histopathology was compared to the pre-operative ultrasound measurements and found no significant association with ultrasound baseline (p=0.197), time to initial rise (p=0.926), inflow (p=0.855), time to peak (p=0.409), peak (p=0.855), or outflow (p=1.000). No significant association was found with intra-operative ultrasound baseline (p=0.855), inflow (p=0.273), time to peak (p=0.521), peak (p=0.715), or outflow (p=0.521), however there was a significant difference associated with the intra-operative ultrasound time to initial rise (p=0.028) indicating a longer time to initial rise was associated with a greater chance of hemorrhage.

The presence of edema on histopathology was not significantly associated with pre-operative ultrasound baseline (p=0.182), time to initial rise (p=0.339), inflow (p=0.186), time to peak (p=0.448), and outflow (p=0.298). There was a significant difference associated with the pre-operative ultrasound peak intensity (p=0.014) indicating a higher peak intensity was associated with a greater chance of edema. No significant association was found with intra-operative ultrasound baseline (p=0.704), time to initial rise (p=0.218), inflow (p=0.257), time to peak (p=0.155), peak (p=0.059), or outflow (p=0.088).

The presence of thrombosis on histopathology was not significantly associated with pre-operative ultrasound baseline (p=0.216), time to initial rise (p=0.256), inflow (p=0.221), peak (p=0.414), or outflow

(p=0.838). A significant difference was found associated with the pre-operative ultrasound time to peak (p=0.04) indicating a faster time to peak was associated with a greater chance of thrombosis. No significant association was found with intra-operative ultrasound baseline (p=0.081), time to initial rise (p=0.184), inflow (p=0.103), peak (p=0.221), or outflow (p=0.412). There was a significance association found with intra-operative ultrasound time to peak (p=0.014) indicating a faster time to peak was associated with a greater chance of thrombosis.

The presence of necrosis on histopathology was not significantly associated with pre-operative ultrasound baseline (p=0.086), time to initial rise (p=0.104), inflow (p=0.059), peak (p=0.257), or outflow (p=0.85). There was a significant difference associated with the pre-operative ultrasound time to peak (p=0.046) indicating a faster time to peak was associated with a greater chance of necrosis. No significant association was found with intra-operative ultrasound time to initial rise (p=0.636), inflow (p=0.186), time to peak (p=0.129), peak (p=0.45), or outflow (p=0.569). There was a significant association with the intra-operative ultrasound baseline (p=0.046) indicating a higher baseline intensity was associated with a greater chance of necrosis.

Ultrasound variables were also evaluated for any association with patient survival. There was a significant association with the subjective assessment of a perfusion deficit on ultrasound and patient mortality (p=0.014) indicating that the presence of a perfusion deficit during subjective assessment of the CEUS exam was associated with a greater chance of patient death (Fig. 7A). No significant association was found with pre-operative ultrasound baseline (p=0.062), time to initial rise (p=0.113), inflow (p=0.056), time to peak (p=0.178), peak (p=0.206), or outflow (p=0.684). No significant association was found with intra-operative ultrasound baseline (p=0.289), time to initial rise (p=0.515), inflow (p=0.44), time to peak (p=0.943), peak (p=0.08), or outflow (p=0.454).

CT data was also analyzed for association with patient survival. There was no significant association between patient mortality and the subjective presence of a perfusion deficit (p=0.166) (Fig. 7B). No significant association was found in the pre-contrast series at the lesion (p=0.156) or orad to the lesion (p=0.95), however there was a significant association between patient mortality and the CT ROI measurements aborad to the lesion (p=0.036, Harrell's C=0.8571) and at normal intestine (p=0.036, Harrell's C=0.9048). Both of these significant findings indicated that a lower HU value was associated with a greater chance of patient death (Fig. 6). For the arterial phase, there was no significant association was found at the lesion (p=0.264), orad to the lesion (p=0.624), aborad to the lesion (p=0.735), or at normal intestine (p=0.132). In the venous phase, there was no significant association found at the lesion (p=0.351), orad to the lesion (p=0.218), aborad to the lesion (p=0.251), or at normal intestine (p=0.385). In the delayed phase, there was no significant association found at the lesion (p=0.762), orad to the lesion (p=0.819), aborad to the lesion (p=0.51), or at normal intestine (p=0.499).

Discussion:

Following suite from a previous study,[111] dogs that required resection and anastomosis had a higher chance of post-operative complications as 3/4 (75%) of cases ultimately died or experienced surgical site dehiscence requiring a second resection procedure. The patient requiring a second resection and anastomosis recovered to be discharged, but the hospitalization period of 9 days was longer than any other patient in the study and cost of care assuredly was high. Interestingly, all patients that required a resection and anastomosis presented with differing underlying gastrointestinal disease. In contrast to a previous study indicating linear foreign bodies had a poorer survival rate,[113] the survival rate between linear and discrete foreign bodies in our study was the same. As only patient in each of the linear and discrete foreign body categories died, numbers are clearly too low to decidedly contradict the previously published trend.

All patients that underwent resection and anastomosis had visual perfusion deficits detected in the small intestine on CEUS, however only 3/4 (75%) were detected on CT. The presence of a visual deficit on CEUS was also highly correlated with predicting which patients would survive (Fig. 7). However, when analyzing the measurements obtained from the CEUS examinations, no objective association for predicting survivability was found. Several explanations for this discrepancy exist. First, the CEUS measurements were taken to include as much of the intestinal wall as possible. This method may have included enough "normal" intestine in the adjacent portions to negate any significant difference. It was decided not to measure the perfusion deficits alone, as it was often impossible to ensure that the perfusion deficit was actually that, and not in reality a portion of the intestinal lumen or adjacent peritoneum, due to the shape and location of the lesions. A second explanation could be reviewer bias. Although one reviewer was blinded to patient history and the other had a minimum of six months between patient exams and image analysis, a consensus agreement could still be swayed inappropriately. In contrast, the presence of a subjective visual deficit on CT was significantly associated with both histopathology ischemia grade and the presence of necrosis. Interestingly, CT measurements obtained at the actual lesion site were not correlated with any histopathology findings. This was an unexpected finding as one would assume that the most dramatic changes in perfusion might exist at the most severely affected portion of bowel. Although no perceived change in degree of difficulty obtaining measurements was noted between sites, measurements may have been more difficult to obtain at the lesion site due to obscured intestinal wall margins. Altered intestinal wall shape secondary to plication, adjacent changes within the peritoneum such as effusion or fat-stranding, or artifact such as beam hardening emanating from a foreign object could all blur intestinal margins.

Few associations which can be immediately clinically applicable were found when reviewing the statistically significant CEUS measurement values. It was interesting to note that the only consistent finding between the pre-operative and intra-operative CEUS exams were that a faster time to peak was associated with a greater chance of thrombosis. Overall both the pre-operative and intra-operative CEUS

had similar quantity of significant associations found, despite our hope that intra-operative examination would be superior. We had theorized that the more definitive intra-operative examination of the affected portion of intestine would in turn produce more accurate results. Perhaps the intra-operative CEUS truly provides no more useful data than a pre-operative study. However, several differences in our project design may account for the lackluster results obtained. First, our examination methods differed slightly from previously published intra-operative CEUS examination of normal small intestine in dogs.[11] The previous study filled the abdomen with saline and had the ultrasound probe submerged with the intestinal loop being interrogated. In our study of diseased patients, several had perforated intestinal segments. Filling the abdomen of these patients with saline and submerging intestinal rents into the fluid could allow bacteria to spread more rapidly and diffusely throughout the abdomen. Instead, it was decided to immediately isolate the affected intestinal loops with sterile gauze in order to minimize abdominal contamination. Although contact between the ultrasound probe and intestine was deemed adequate at the time, perhaps a difference truly existed. A second difference in project design included a change in the contrast dose administered intra-operatively. In the previous paper[11] 0.03ml/kg was determined to be the optimal contrast dose. However, these patients were only receiving the intra-operative examinations. In our study, as two exams were performed and the majority of examinations required multiple contrast injections, it was decided to use the published standard exam dose[69] for both exams for several factors. First, any chance to reduce the contrast exposure to each patient was pursued as the potential for allergic reaction, albeit low, has been reported.[14] Second, using the 0.03ml/kg dose intra-operatively would result in a much larger quantity of contrast being administered to each patient, not only increases drug exposure risk but also increases supply cost. Lastly, standardizing the dose between examinations would eliminate any possible change in pixel intensity based on dose discrepancies.

In this study, we were able to uncover several interesting trends in the pre-contrast CT. HU measurements obtained at both the aborad and normal intestinal sites were significantly correlated with survival. These changes could be interpreted two ways: either lower HU values were associated with a

higher chance of death or higher HU values were associated with a higher chance of survival. To the author's knowledge, no published normal HU values for canine small intestine exist. In order to determinate which interpretation should be accepted, comparison to values obtained from canine patients that have no known gastrointestinal disease should be performed. The pre-contrast aborad segments were also significantly associated with ischemia grade and presence of thrombosis. Lower HU values were associated with an increased chance of both histopathology changes. Although the overall number of significant associations between pre-contrast CT exams and histopathology changes was not higher than any specific post-contrast phase, the clinical significance of these changes was potentially greater. Intravenous administration of CT contrast agents is contraindicated in dehydrated patients. As many patients presenting with gastrointestinal disease may be exhibiting vomiting or diarrhea, dehydration may be a common sequela. Performing a solely pre-contrast CT exam would avoid any potential contrast-associated risks.

There were several limitations of this study. First, the number of patients recruited was low. Although the patient enrollment period was open for a number of months after the last dog was enrolled, no additional qualifying patients were admitted to the hospital and successfully recruited. One factor in the low recruitment numbers was wariness exhibited by the clients as to potential risks of either the CT or US contrast agents. A variety of clinicians participated in patient recruitment, ranging from beginning rotating interns to final year specialty residents, and perhaps having one advanced level of clinicians responsible for recruitment would increase client participation.

A second limitation was the distribution of primary disease among patients and low numbers of patients requiring intestinal resections. As this study required patients to undergo study recruitment prior to knowing the full extent of surgical intervention required, it was assumed a portion of patients would only require an enterotomy. Many of the patients that would have been ideal study candidates, such as those

with gastrointestinal neoplasia, were not able to be recruited due to a poor to grave prognosis and clients instead often opted for euthanasia.

There were also several limitations in our experimental methods. First, there were no healthy controls. Instead each animal was used as its own control. Limited amounts of data were available from the two patients recruited which did not require an enterotomy and instead received a gastrotomy. However, performing an intestinal biopsy in patients in which one was not clinically indicated would not be considered ethical. No interobserver analysis was performed for the measurements obtained. Over 4000 measurements were manually obtained in this study. As performing agreement analysis or determining interobserver measurement accuracy were not within our study objectives, it was seemingly not worthwhile to have multiple observers perform such a tedious and time-consuming task. As patients varied between awake, sedated, and anesthetized for different portions of the study, individual patient parameters such as blood pressure could not be standardized. Future studies may consider monitoring blood pressure during the pre-operative imaging in order to eliminate systemic hypo- or hypertension as a variable which may affect perfusion.

The CEUS exam was limited in several ways. Ideally we would have interrogated multiple areas within the gastrointestinal tract to correspond to the orad, aborad, and normal areas analyzed on CT, with 1-2 injections performed at each site. However, although the maximum number of contrast injections able to be performed within a restricted timeframe has not been established, common practice is to limit them to a reasonable amount and frequently we have found 1-3 injections are performed for a complete exam. When performing multiple injections in both the pre-operative and intra-operative timeframes, which often were sequential and separated by a matter of hours, it became necessary to limit the number of injections for each study to only interrogate the lesion site. This also helped limit excessive time under general anesthesia during the intra-operative exam. Although a standardized dose was used for the pre-operative and intra-operative CEUS exams, the intra-operative dose chosen was lower than the

recommended dose previously published.[11] In this previous study, they also found that the pixel intensity increased as the contrast dose increased, so using the standard CEUS dose for the pre-operative exam and following this with a potentially larger dose intra-operatively would have directly affected the time intensity curve data collected. If the 0.03ml/kg dose was used for both CEUS exams, this would have dramatically increased the volume of contrast and subsequently the cost of contrast agent per patient, particularly when repeated injections were performed. For the larger patients enrolled in this study, this could have potentially doubled the research costs appropriated for each patient and further limited the amount of overall patients able to be enrolled.

Finally several artifacts were observed during CT that may influence the HU measurements (Fig. 8). Several patients had hyperattenuating objects (i.e. rocks) within the intestine that resulted in beam hardening artifact, most severe at the site of the lesion. However, this would affect each CT series equally, so its effect should be minimized. As patients were sedated for the CT exam, respiratory motion was also observed. If using general anesthesia, hyperventilating the patient immediately prior to the scan or performing a breath hold are two methods frequently employed to limit respiratory motion. Respiratory motion can result in blurring of organs. In this case, defining the intestinal wall borders could become more challenging. Every effort was made to choose an image slice at the same level between each series that minimized any respiratory motion while still corresponding to the areas of interest.

A number of future directions should be considered to continue to investigate gastrointestinal ischemia in dogs. First, as a subjective visual perfusion deficit was highly associated with predicting patient survival, further analysis may include both quantifying the number of deficits visualized and measuring each deficit to determine which factors more into the perception of a deficit existing. Ideally, the interrogated region of small intestine would be resected and ischemic areas would be measured on histopathology for correlation to the ultrasound measurements obtained. As no adverse reactions were observed in the patients participating in this study, future researchers may elect to perform a higher number of contrast

injections for each patient. This would allow multiple segments of small intestine to be thoroughly interrogated, particularly those adjacent to the site of the lesion, as CT measurements found numerous histopathologic associations at the orad, aborad, and normal segments. Future intra-operative CEUS studies interrogating the small intestine may also investigate whether direct injection of the contrast into a mesenteric artery may improve image quality. Finally, continued investigation into the validity for performing a survey CT to predict patient survival is warranted. Comparison between CT ROI measurements performed in those with and without underlying gastrointestinal disease should also be performed.

In conclusion, multiple imaging findings obtained from CT were correlated with intestinal ischemia grade while numerous other findings on both CT and CEUS were correlated with a variety of other histopathologic features. Both the assessment of a perfusion deficit on CEUS and several measurements obtained from survey CT were highly predictive of patient survival. Overall no advantage of performing an intra-operative CEUS exam was appreciated. Further investigation into the clinical utility of these imaging applications for the assessment of gastrointestinal perfusion and ischemia is warranted.

CHAPTER 3

FIGURES AND TABLES

Figure 1:

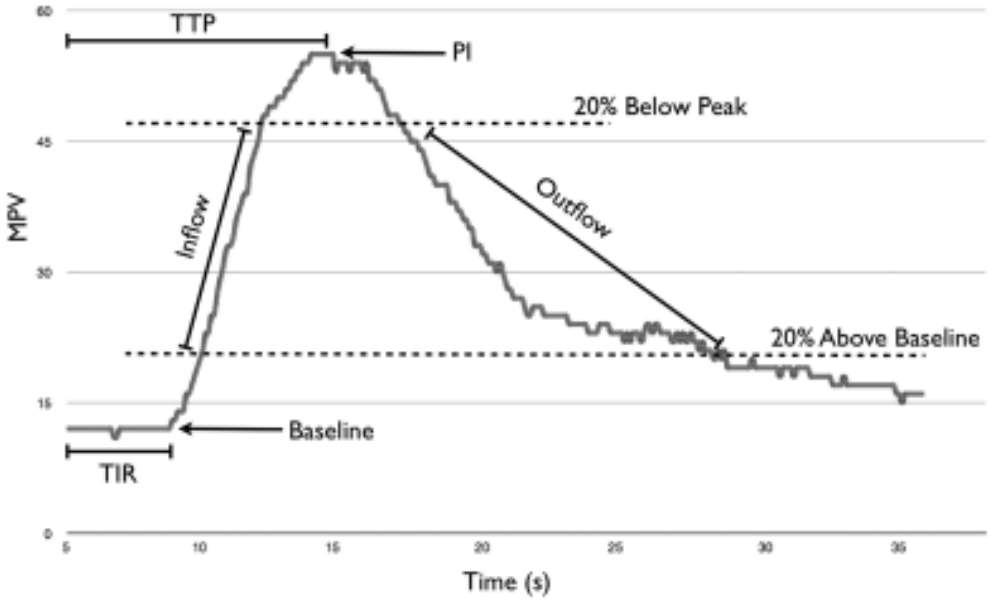

Representative time-intensity curve collimated to the time period of visible contrast enhancement. The baseline mean pixel value (MPV) is unchanged throughout the time to initial rise (TIR). Contrast enhancement increases during inflow until reaching peak intensity (PI). Time to peak (TTP) is the time from injection to the PI. Outflow of contrast medium is more gradual than inflow.[11]

Figure 2:

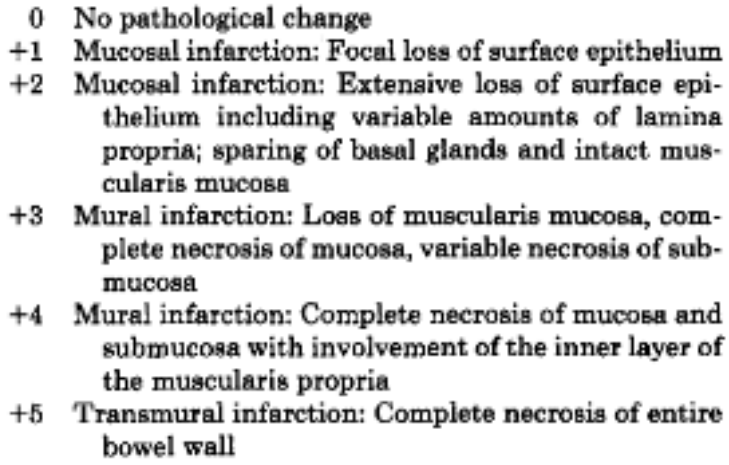

0	No pathological change
+1	Mucosal infarction: Focal loss of surface epithelium
+2	Mucosal infarction: Extensive loss of surface epithelium including variable amounts of lamina propria; sparing of basal glands and intact muscularis mucosa
+3	Mural infarction: Loss of muscularis mucosa, complete necrosis of mucosa, variable necrosis of submucosa
+4	Mural infarction: Complete necrosis of mucosa and submucosa with involvement of the inner layer of the muscularis propria
+5	Transmural infarction: Complete necrosis of entire bowel wall

Histopathologic classification scheme used for evaluation of degree of bowel necrosis.[119]

Figure 3:

A:

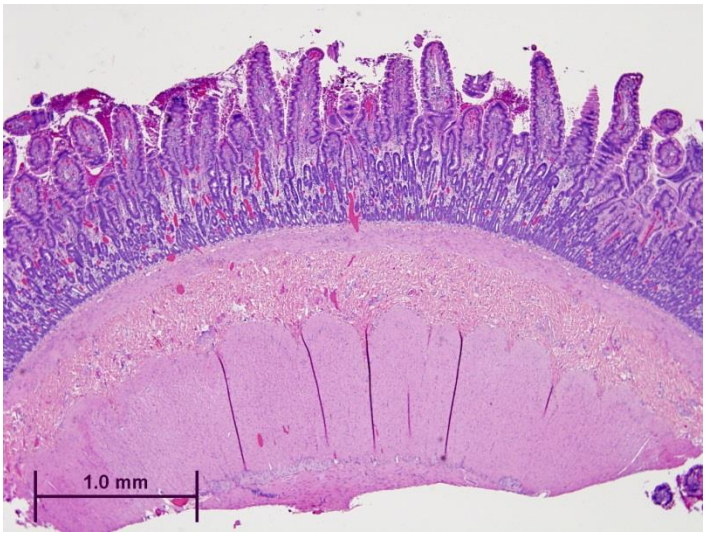

B:

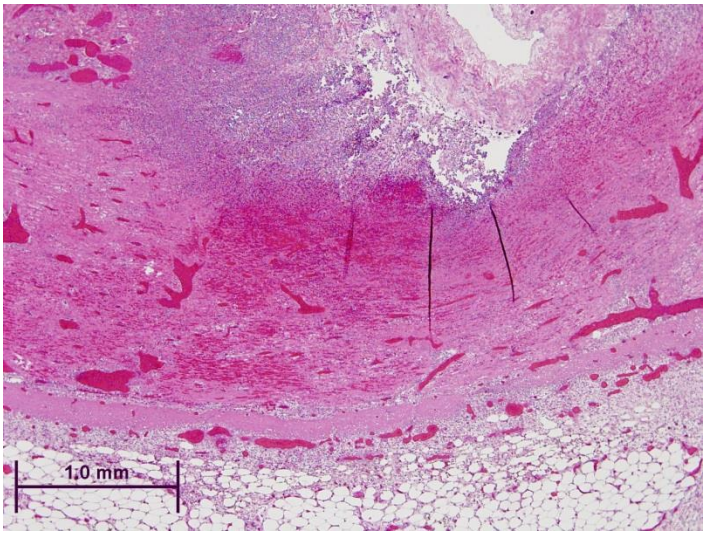

Histopathology samples observed at 4x. A) Intestinal biopsy obtained from patient 9 demonstrating a histopathology score of 0. B) Intestinal resection sample obtained from patient 2 demonstrating a histopathology score of 4.

Figure 4:

A:

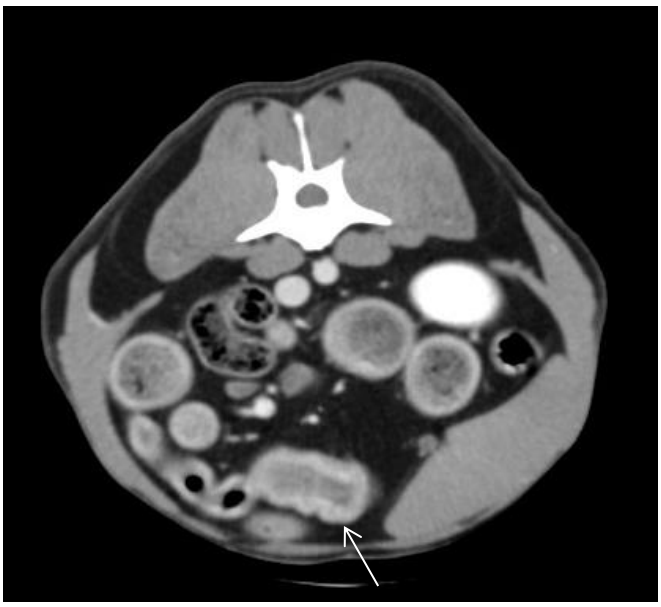

B:

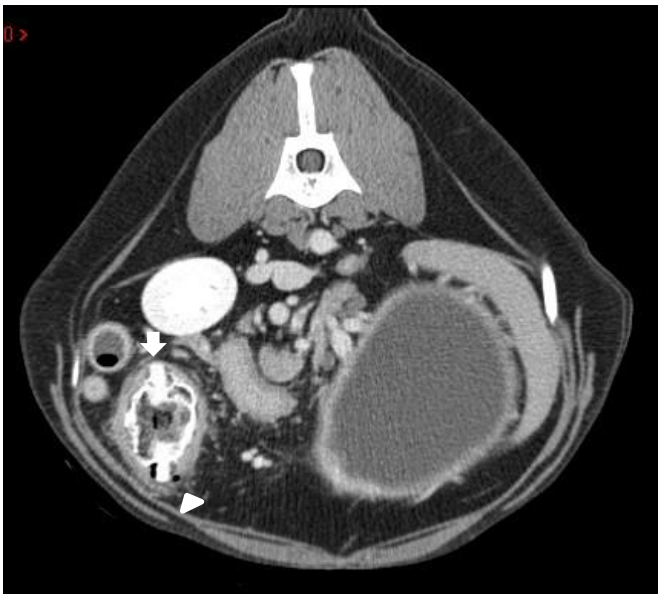

Post-contrast transverse CT images. The patient's right is to the reader's left. A) Section of plicated small intestine in patient 11 demonstrating normal wall enhancement (long arrow). B) Hyperattenuating luminal foreign material at the site of intestinal obstruction (short arrow) in patient 2. At this same level, a focal area of non-enhancing intestinal wall is observed and gas can be seen crossing the intestinal wall (arrowhead).

Figure 5:

A:

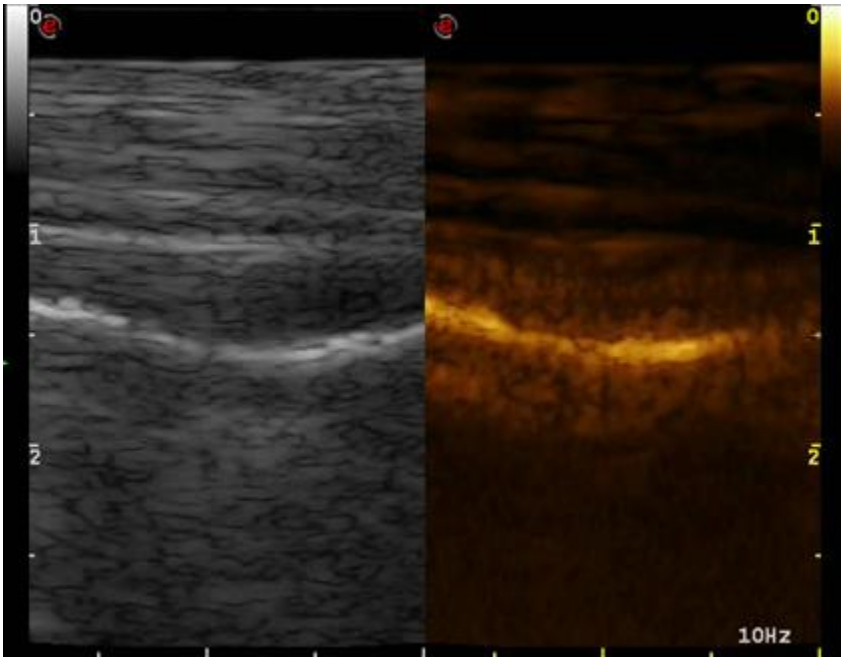

B:

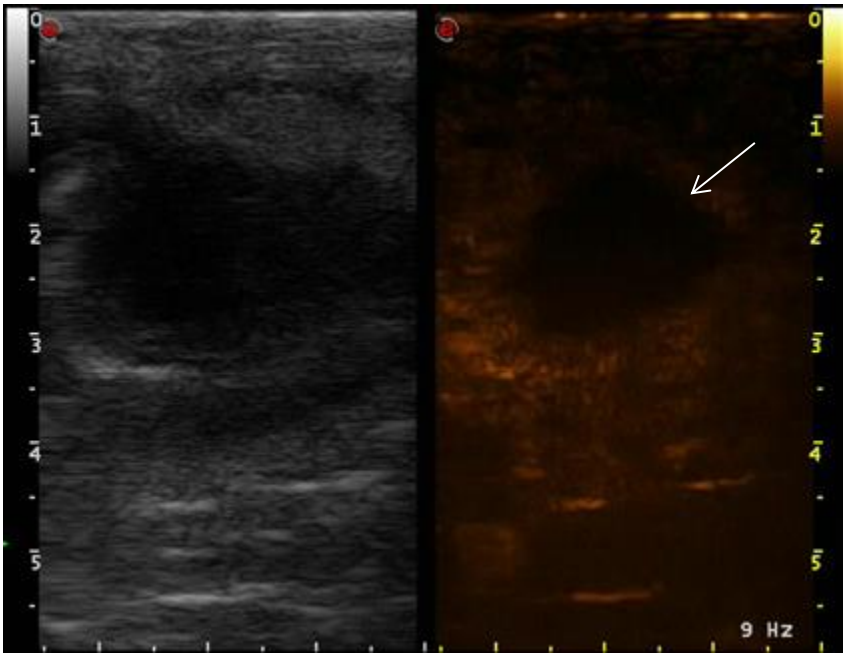

Examples of CEUS exams. Gray-scale image on the reader's left and CEUS image on the reader's right. A) Small intestine in patient 12, demonstrating normal homogenous contrast dispersal. B) Small intestine in patient 4, demonstrating a large hypoechoic lesion within the small intestinal wall on gray-scale that is non-perfusing on CEUS (long arrow).

Figure 6:

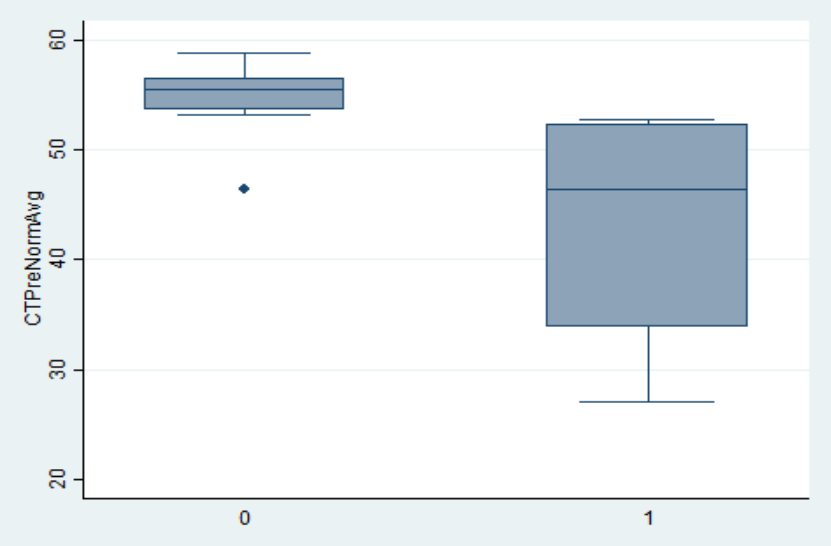

Bar graph comparing patient survival with CT measurements. Patients that survived had a significantly higher HU measurement obtained in the pre-contrast CT series at the site of normal intestine. Patients that died had a lower HU measurement. (CTPreNormAvg = HU average obtained from the pre-contrast CT at the site of normal intestine; 0 = patients that lived; 1 = patients that died)

Figure 7:

A:

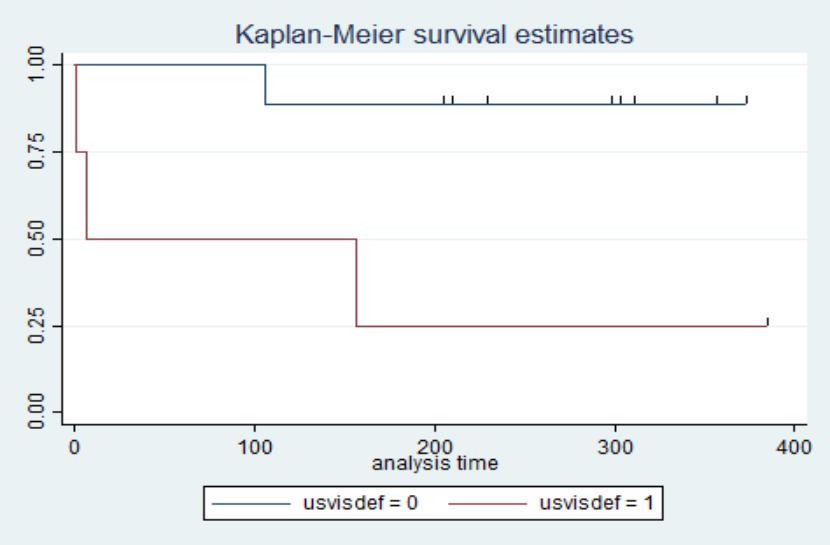

B:

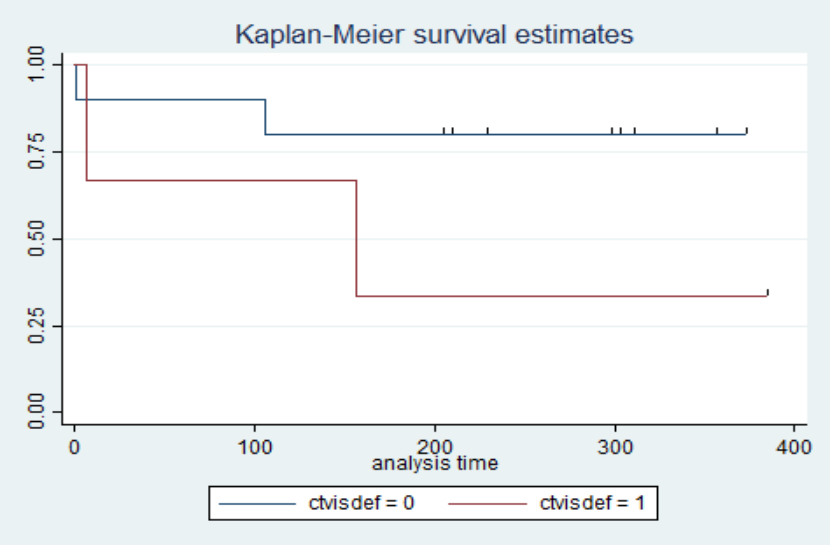

Kaplan-Meier survival plots. A) The subjective presence of a perfusion deficit on CEUS was associated with patient death. B) The subjective presence of a perfusion deficit on CT was not predictive of patient survival. (usvisdef = 0 indicates no deficit observed; usvisdef = 1 indicates a deficit was observed; ctvisdef = 0 indicates no deficit observed; ctvisdef = 1 indicates a deficit was observed)

Figure 8:

A:

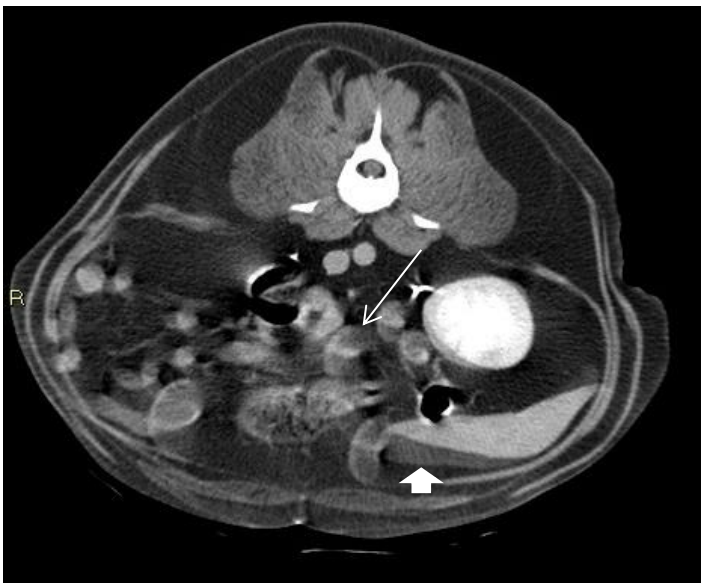

B:

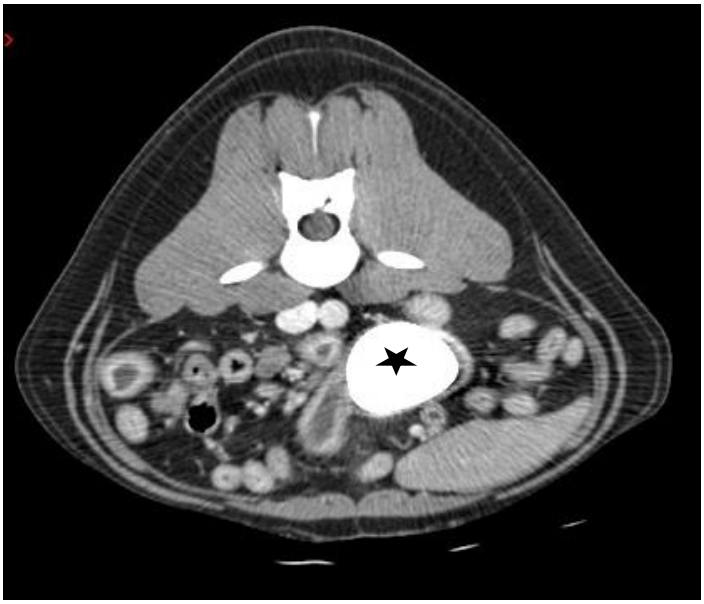

Transverse post-contrast CT images demonstrating several artifacts. A) Motion artifact observed in patient 7 resulting in blurring (long arrow) and duplication (short arrow) of organ margins. B) A strongly hyperattenuating object (star) is located within the small intestine of patient 12 resulting in beam hardening artifact, visible as alternating hyperattenuating and hypoattenuating lines radiating from the object.

Table 1:

Patient number	Type	Procedure	Site	Complications	Days hospitalized	Date of death
1	Linear with intussusception	Resection	Jejunum	Cardiac arrest	2	2
2	Discrete	Resection	Jejunum	____	5	__
3	Linear	Biopsy	Stomach	Fever and incisional drainage	5	__
4	Abscess	Resection	Jejunum	Surgical site dehiscence	9	158
5	Linear	Biopsy	Jejunum	____	2	__
6	Discrete	Biopsy	Jejunum	____	3	__
7	Discrete	Biopsy	Jejunum	____	3	107
8	Linear	Biopsy	Jejunum	____	3	__
9	Discrete	Biopsy	Jejunum	____	3	__
10	Discrete	Biopsy	Jejunum	____	3	__
11	Linear	Biopsy	Stomach	____	3	__
12	Discrete	Biopsy	Jejunum	____	2	__
13	Neoplasia	Resection	Ileocolic junction	Septic abdominal effusion	8	8

Summary of presenting conditions, surgical procedure performed, and post-operative data.

Table 2:

Patient number	Ischemia grade	Necrosis	Thrombosis	Edema	Hemorrhage	Ulceration/erosion	Inflammation
1	5	Yes	Yes	Yes	No	Yes	Yes
2	4	Yes	No	No	Yes	Yes	Yes
3	—	—	—	—	—	—	—
4	5	Yes	Yes	No	Yes	Yes	Yes
5	1	No	No	No	Yes	Yes	No
6	1	No	No	No	Yes	Yes	Yes
7	0	No	No	No	Yes	No	No
8	0	No	No	No	No	No	No
9	0	No	No	Yes	No	No	No
10	0	No	No	Yes	No	No	Yes
11	—	—	—	—	—	—	—
12	0	No	No	No	No	No	No
13	5	Yes	Yes	Yes	Yes	Yes	Yes

Summary of histopathology findings.

CHAPTER 4

REFERENCES

1. Armstrong WF. Assessment of myocardial perfusion with contrast enhanced echocardiography. Echocardiography. 1986;3:355–370.

2. Feinstein SB. Contrast echocardiography: An introduction. Clin Cardiol. 1991;14:V-1–V-3.

3. Szatmári V, Harkaanyi Z, Vöaröas K. A review of nonconventional ultrasound techniques and contrast-enhanced ultrasonography of noncardiac canine disorders. Vet Radiol Ultrasound. 2003;44:380–391.

4. Schmid V, Lang J. Intravascular ultrasound contrast media. Vet Radiol Ultrasound. 1995;36:307–314.

5. Bahr A, Wrigley R, Salman M. Quantitative evaluation of Imagent® as an abdominal ultrasound contrast medium in dogs. Vet Radiol Ultrasound. 2000;41:50–55.

6. Correas JM, Bridal L, Lesavre A, et al. Ultrasound contrast agents: properties, principles of action, tolerance, and artifacts. Eur Radiol. 2001;11:1316-1328.

7. Wilson SR, Greenbaum LD, Goldberg BB. Contrast-enhanced ultrasound: what is the evidence and what are the obstacles? Am J Roentgenol. 2009 Jul;193:55–60.

8. Alzaraa A, Gravante G, Chung WY, et al. Contrast-enhanced ultrasound in the preoperative, intraoperative and postoperative assessment of liver lesions. Hepatol Res. 2013;43:809–819.

9. Martin KH, Dayton PA. Current status and prospects for microbubbles in ultrasound theranostics. Wiley Interdiscip Rev Nanomed Nanobiotechnol. 2013;5:329–345.

10. Mullin L, Gessner R, Kwan J, Kaya M, Borden MA, Dayton PA. Effect of anesthesia carrier gas on in vivo circulation times of ultrasound microbubble contrast agents in rats. Contrast Media Mol Imaging. 2011 May;6:126–131.

11. Jiménez DA, O'Brien RT, Wallace JD, Klocke E. Intraoperative contrast-enhanced ultrasonography of normal canine jejunum. Vet Radiol Ultrasound. 2011;52:196–200.

12. Leinonen MR, Raekallio MR, Vainio OM, Ruohoniemi MO, O'Brien RT. The effect of the sample size and location on contrast ultrasound measurement of perfusion parameters. Vet Radiol Ultrasound. 2011;52:82–87.

13. Wei K, Mulvagh SL, Carson L, et al. The safety of Definity and Optison for ultrasound image enhancement: a retrospective analysis of 78,383 administered contrast doses. J Am Soc Echocardiogr. 2008 Nov;21:1202–1206.

14. Seiler G, Brown J, Reetz J, et al. Safety of contrast-enhanced ultrasonography in dogs and cats: 488 cases (2002-2011). J Am Vet Med Assoc. 2013;242:1255-1259.

15. Sieswerda GT, Kamp O, Visser CA. Myocardial contrast echocardiography: clinical benefit and practical issues. Echocardiography. 2000;17:s25–s36.

16. Cianciulli TF, Lax JA, Beck MA, et al. Usefulness of myocardial contrast echocardiography early after acute myocardial infarction. Echocardiography. 2006;23:208–217.

17. Giannoni MF, Irace L, Vicenzini E, Massa R, Gossetti B, Benedetti-Valentini F. Carotid body tumors: advantages of contrast ultrasound investigation. J Neuroimaging. 2009;19:388–390.

18. Huang P, Huang F, Zou C, et al. Contrast-enhanced sonographic characteristics of neovascularization in carotid atherosclerotic plaques. J Clin Ultrasound. 2008;36:346–351.

19. Azevedo EI, Castro PM. Novel Applications of Ultrasound Vascular Imaging. Vascular imaging of the central nervous system. John Wiley & Sons, Ltd. 2014;33–66.

20. Piscaglia F, Bolondi L. Recent advances in the diagnosis of hepatocellular carcinoma. Hepatol Res. 2007;37:S178–S192.

21. Liu L-P, Dong B-W, Yu X-L, Zhang D-K, Kang C-S, Zhao X-H. Evaluation of focal fatty infiltration of the liver using color Doppler and contrast-enhanced sonography. J Clin Ultrasound. 2008;36:560–566.

22. Von Herbay A, Westendorff J, Gregor M. Contrast-enhanced ultrasound with SonoVue: differentiation between benign and malignant focal liver lesions in 317 patients. J Clin Ultrasound. 2010;38:1–9.

23. Yoshizumi H, Maruyama H, Okugawa H, et al. How to characterize non-hypervascular hepatic nodules on contrast-enhanced computed tomography in chronic liver disease: feasibility of contrast-enhanced ultrasound with a microbubble contrast agent. J Gastroenterol Hepatol. 2008 Oct;23:1528–1534.

24. Wang J-H, Lu S-N, Hung C-H, et al. Small hepatic nodules (≤2 cm) in cirrhosis patients: characterization with contrast-enhanced ultrasonography. Liver Int. 2006;26:928–934.

25. Maruyama H, Takahashi M, Ishibashi H, et al. Ultrasound-guided treatments under low acoustic power contrast harmonic imaging for hepatocellular carcinomas undetected by B-mode ultrasonography. Liver Int. 2009;29:708–714.

26. Sugimoto K, Moriyasu F, Kamiyama N, et al. Analysis of morphological vascular changes of hepatocellular carcinoma by microflow imaging using contrast-enhanced sonography. Hepatol Res. 2008;38:790–799.

27. Cobbold JFL, Patel D, Fitzpatrick JA, et al. Accuracy and reliability of microbubble ultrasound measurements for the non-invasive assessment of hepatic fibrosis in chronic hepatitis C: transit time comparison in hepatitis C. Hepatol Res. 2012 May;42:515–522.

28. Iijima H, Moriyasu F, Tsuchiya K, et al. Decrease in accumulation of ultrasound contrast microbubbles in non-alcoholic steatohepatitis. Hepatol Res. 2007;37:722–730.

29. Agrawal N, Fowler AL, Thomas MG. The routine use of intra-operative ultrasound in patients with colorectal cancer improves the detection of hepatic metastases. Colorectal Dis. 2006;8:192–194.

30. Mazzoni G, Napoli A, Mandetta S, et al. Intra-operative ultrasound for detection of liver metastases from colorectal cancer. Liver Int. 2008;28:88–94.

31. Hardy K, Martin J, Fletcher D, Maclellan D, Jones R. Hepatic resection: value of operative ultrasound and ultrasonic dissection. Aust N Z J Surg. 1989;59:621–623.

32. Viganò L, Ferrero A, Amisano M, Russolillo N, Capussotti L. Comparison of laparoscopic and open intraoperative ultrasonography for staging liver tumours. Br J Surg. 2013;100:535–542.

33. Leroux PD, Winter TC, Berger MS, Mack LA, Wang K, Elliott JP. A comparison between preoperative magnetic resonance and intraoperative ultrasound tumor volumes and margins. J Clin Ultrasound. 1994;22:29–36.

34. Shah AJ, Callaway M, Thomas MG, Finch-Jones MD. Contrast-enhanced intraoperative ultrasound improves detection of liver metastases during surgery for primary colorectal cancer. HPB. 2010;12:181–187.

35. Martin RCG, Reuter NP, Woodall C. Intra-operative contrast-enhanced ultrasound improves image enhancement in the evaluation of liver tumors. J Surg Oncol. 2010;101:370–375.

36. Klauser A, Frauscher F, Schirmer M, et al. The value of contrast-enhanced color doppler ultrasound in the detection of vascularization of finger joints in patients with rheumatoid arthritis. Arthritis Rheum. 2002;46:647–653.

37. Stramare R, Raffeiner B, Ciprian L, et al. Evaluation of finger joint synovial vascularity in patients with rheumatoid arthritis using contrast-enhanced ultrasound with water immersion and a stabilized probe. J Clin Ultrasound. 2012;40:147–154.

38. Mitterberger M, Pinggera GM, Colleselli D, et al. Acute pyelonephritis: comparison of diagnosis with computed tomography and contrast-enhanced ultrasonography. BJU Int. 2008;101:341–344.

39. Qi TY, Chen YQ, Jiang J, Zhu YK, Yao XH, Qi J. Contrast-enhanced transrectal ultrasonography: Measurement of prostate cancer tumor size and correlation with radical prostatectomy specimens. Int J Urol. 2013;20:1085–1091.

40. Aigner F, Pallwein L, Mitterberger M, et al. Contrast-enhanced ultrasonography using cadence-contrast pulse sequencing technology for targeted biopsy of the prostate. BJU Int. 2009;103:458–463.

41. Eckersley RJ, Sedelaar JPM, Blomley MJK, et al. Quantitative microbubble enhanced transrectal ultrasound as a tool for monitoring hormonal treatment of prostate carcinoma. The Prostate. 2002;51:256–267.

42. Sedelaar JPM, van Leenders GJLH, Goossen TEB, et al. Value of contrast ultrasonography in the detection of significant prostate cancer: Correlation with radical prostatectomy specimens. The Prostate. 2002;53:246–253.

43. Zhou L, Zhang X, Chen X, et al. Value of three-dimensional hysterosalpingo-contrast sonography with SonoVue in the assessment of tubal patency. Ultrasound Obstet Gynecol. 2012;40:93–98.

44. Testa AC, Timmerman D, Van Belle V, et al. Intravenous contrast ultrasound examination using contrast-tuned imaging (CnTI™) and the contrast medium SonoVue® for discrimination between benign and malignant adnexal masses with solid components. Ultrasound Obstet Gynecol. 2009;34:699–710.

45. Hamada T, Yamauchi M, Tanaka M, Hashimoto Y, Nakai K, Suenaga K. Prospective evaluation of contrast-enhanced ultrasonography with advanced dynamic flow for the diagnosis of intestinal ischaemia. Br J Radiol. 2007 Aug;80:603–608.

46. Hata J, Kamada T, Haruma K, Kusunoki H. Evaluation of bowel ischemia with contrast-enhanced US: initial experience. Radiology. 2005 Aug;236:712–715.

47. Kanzaki T, Hata J, Imamura H, et al. Contrast-enhanced ultrasonography with Sonazoid™ for the evaluation of bowel ischemia. J Med Ultrason. 2012 Jul;39:161–167.

48. Giannetti A, Biscontri M, Randisi P, Cortese B, Minacci C, Stumpo M. Contrast-enhanced sonography in the diagnosis of acute mesenteric ischemia: case report. J Clin Ultrasound. 2009; 156-160.

49. Tobin L, Simonsen L, Bülow J. Real-time contrast-enhanced ultrasound determination of microvascular blood volume in abdominal subcutaneous adipose tissue in man. Evidence for adipose tissue capillary recruitment. Clin Physiol Funct Imaging. 2010;30:447–452.

50. Mulder AH, van Dijk APJ, Smits P, Tack CJ. Real-time contrast imaging: a new method to monitor capillary recruitment in human forearm skeletal muscle. Microcirculation. 2008 Jan;15:203–213.

51. Wong KK, Huang I, Kim YR, et al. In vivo study of microbubbles as an MR susceptibility contrast agent. Magn Reson Med. 2004;52:445–452.

52. Alexander AL, McCreery TT, Barrette TR, Gmitro AF, Unger EC. Microbubbles as novel pressure-sensitive MR contrast agents. Magn Reson Med. 1996;35:801–806.

53. Peng S-L, Wang F-N, Wang C-H, Peng H-H, Lu C-T, Yeh C-K. Using microbubbles as an MRI contrast agent for the measurement of cerebral blood volume. NMR Biomed. 2013;26:1540–1546.

54. Lindner JR, Kaul S. Delivery of drugs with ultrasound. Echocardiography. 2001;18:329–337.

55. Tinkov S, Bekeredjian R, Winter G, Coester C. Microbubbles as ultrasound triggered drug carriers. J Pharm Sci. 2009;98:1935–1961.

56. Klibanov AL, Rychak JJ, Yang WC, et al. Targeted ultrasound contrast agent for molecular imaging of inflammation in high-shear flow. Contrast Media Mol Imaging. 2006;1:259–266.

57. Ottoboni S, Short RE, Kerby MB, Tickner EG, Steadman E, Ottoboni TB. Characterization of the in vitro adherence behavior of ultrasound responsive double-shelled microspheres targeted to cellular adhesion molecules. Contrast Media Mol Imaging. 2006;1:279–290.

58. Weller GER, Villanueva FS, Tom EM, Wagner WR. Targeted ultrasound contrast agents: in vitro assessment of endothelial dysfunction and multi-targeting to ICAM-1 and sialyl Lewisx. Biotechnol Bioeng. 2005;92:780–788.

59. Wang L, Li L, Guo Y, et al. Construction and in vitro/in vivo targeting of PSMA-targeted nanoscale microbubbles in prostate cancer. The Prostate. 2013;73:1147–1158.

60. Hettiarachchi K, Zhang S, Feingold S, Lee AP, Dayton PA. Controllable microfluidic synthesis of multiphase drug-carrying lipospheres for site-targeted therapy. Biotechnol Prog. 2009;25:938–945.

61. Burke CW, Hsiang Y-HJ, Alexander E, Kilbanov AL, Price RJ. Covalently linking poly(lactic-co-glycolic acid) nanoparticles to microbubbles before intravenous injection improves their ultrasound-targeted delivery to skeletal muscle. Small. 2011;7:1227–1235.

62. Chappell JC, Price RJ. Targeted therapeutic applications of acoustically active microspheres in the microcirculation. Microcirculation. 2006;13:57–70.

63. Deckers R, Rome C, Moonen CTW. The role of ultrasound and magnetic resonance in local drug delivery. J Magn Reson Imaging. 2008;27:400–409.

64. Watanabe Y, Aoi A, Horie S, et al. Low-intensity ultrasound and microbubbles enhance the antitumor effect of cisplatin. Cancer Sci. 2008;99:2525–2531.

65. Salwei RM, O'Brien RT, Matheson JS. Use of contrast harmonic ultrasound for the diagnosis of congenital portosystemic shunts in three dogs. Vet Radiol Ultrasound. 2003;44:301–305.

66. Ziegler LE, O'Brien RT, Waller KR, Zagzebski JA. Quantitative contrast harmonic ultrasound imaging of normal canine liver. Vet Radiol Ultrasound. 2003;44:451–454.

67. Nyman HT, Kristensen AT, Flagstad A, McEvoy FJ. A review of the sonographic assessment of tumor metastases in liver and superficial lymph nodes. Vet Radiol Ultrasound. 2004;45:438–448.

68. Nyman HT, Kristensen AT, Kjelgaard-Hansen M, McEvoy FJ. Contrast-enhanced ultrasonography in normal canine liver. Evaluation of imaging and safety parameters. Vet Radiol Ultrasound. 2005;46:243–250.

69. O'Brien RT, Iani M, Matheson J, Delaney F, Young K. Contrast harmonic ultrasound of spontaneous liver nodules in 32 dogs. Vet Radiol Ultrasound. 2004;45:547–553.

70. O'Brien RT. Improved detection of metastatic hepatic hemangiosarcoma nodules with contrast ultrasound in three dogs. Vet Radiol Ultrasound. 2007;48:146–148.

71. Kanemoto H, Ohno K, Nakashima K, et al. Characterization of canine focal liver lesions with contrast-enhanced ultrasound using a novel contrast agent—Sonazoid. Vet Radiol Ultrasound. 2009;50:188–194.

72. Nakamura K, Takagi S, Sasaki N, et al. Contrast-enhanced ultrasonography for characterization of canine focal liver lesions. Vet Radiol Ultrasound. 2010;51:79–85.

73. Ohlerth S, Rüefli E, Poirier V, Roos M, Kaser-Hotz B. Contrast harmonic imaging of the normal canine spleen. Vet Radiol Ultrasound. 2007;48:451–456.

74. Nakamura K, Sasaki N, Yoshikawa M, et al. Quantitative contrast-enhanced ultrasonography of canine spleen. Vet Radiol Ultrasound. 2009;50:104–108.

75. Ohlerth S, Dennler M, Rüefli E, et al. Contrast harmonic imaging characterization of canine splenic lesions. J Vet Intern Med. 2008;22:1095–1102.

76. Rossi F, Leone VF, Vignoli M, Laddaga E, Terragni R. Use of contrast-enhanced ultrasound for characterization of focal splenic lesions. Vet Radiol Ultrasound. 2008;49:154–164.

77. Taeymans O, Penninck D. Contrast enhanced sonographic assessment of feeding vessels as a discriminator between malignant vs. benign focal splenic lesions. Vet Radiol Ultrasound. 2011;52:457–461.

78. Salwei RM, O'Brien RT, Matheson JS. Characterization of lymphomatous lymph nodes in dogs using contrast harmonic and power doppler ultrasound. Vet Radiol Ultrasound. 2005;46:411–416.

79. Gaschen L, Angelette N, Stout R. Contrast-enhanced harmonic ultrasonography of medial iliac lymph nodes in healthy dogs. Vet Radiol Ultrasound. 2010;51:634–637.

80. Gelb HR, Freeman LJ, Rohleder JJ, Snyder PW. Feasibility of contrast-enhanced ultrasound-guided biopsy of sentinel lymph nodes in dogs. Vet Radiol Ultrasound. 2010;51:628–633.

81. Waller KR, O'Brien RT, Zagzebski JA. Quantitative contrast ultrasound analysis of renal perfusion in normal dogs. Vet Radiol Ultrasound. 2007;48:373–377.

82. Kinns J, Aronson L, Hauptman J, Seiler G. Contrast-enhanced ultrasound of the feline kidney. Vet Radiol Ultrasound. 2010;51:168–172.

83. Haers H, Vignoli M, Paes G, et al. Contrast harmonic ultrasonographic appearance of focal space-occupying renal lesions. Vet Radiol Ultrasound. 2010;51:516–522.

84. Haers H, Smets P, Pey P, Piron K, Daminet S, Saunders JH. Contrast harmonic ultrasound appearance of consecutive percutaneous renal biopsies in dogs. Vet Radiol Ultrasound. 2011;52:640–647.

85. Pey P, Vignoli M, Haers H, Duchateau L, Rossi F, Saunders JH. Contrast-enhanced ultrasonography of the normal canine adrenal gland. Vet Radiol Ultrasound. 2011;52:560–567.

86. Bargellini P, Orlandi R, Paloni C, et al. Contrast-enhanced ultrasonographic characteristics of adrenal glands in dogs with pituitary-dependent hyperadrenocorticism. Vet Radiol Ultrasound. 2013;54:283–292.

87. Vanderperren K, Haers H, der Vekens EV, et al. Description of the use of contrast-enhanced ultrasonography in four dogs with pancreatic tumours. J Small Anim Pract. 2013 Oct;1-6.

88. Streitberger A, Hocke V, Modler P. Measurement of pulmonary transit time in healthy cats by use of ultrasound contrast media "Sonovue®": feasibility, reproducibility, and values in 42 cats. J Vet Cardiol. 2013 Sep;15:181–187.

89. Labruyere JJ, Hartley C, Holloway A. Contrast-enhanced ultrasonography in the differentiation of retinal detachment and vitreous membrane in dogs and cats. J Small Anim Pract. 2011;52:522–530.

90. Bigliardi E, Ferrari L. Contrast-enhanced ultrasound of the normal canine prostate gland. Vet Radiol Ultrasound. 2011;52:107–110.

91. Volta A, Manfredi S, Vignoli M, et al. Use of contrast-enhanced ultrasonography in chronic pathologic canine testes. Reprod Domest Anim. 2013;1-8.

92. Diana A, Specchi S, Baron Toaldo M, Chiocchetti R, Laghi A, Cipone M. Contrast-enhanced ultrasonography of the small bowel in healthy cats. Vet Radiol Ultrasound. 2011;52:555–559.

93. Angelelli G, Scardapane A, Memeo M, Stabile Ianora AA, Rotondo A. Acute bowel ischemia: CT findings. Eur J Radiol. 2004 Apr;50:37–47.

94. Reginelli A, Genovese E, Cappabianca S, et al. Intestinal ischemia: US-CT findings correlations. Crit Ultrasound J. 2013 Jul 15;5:S7.

95. Furukawa A, Kanasaki S, Kono N, et al. CT diagnosis of acute mesenteric ischemia from various causes. Am J Roentgenol. 2009 Feb;192:408–416.

96. Wiesner W, Khurana B, Ji H, Ros PR. CT of acute bowel ischemia. Radiology. 2003 Mar;226:635–650.

97. Panés J, Piqué JM. Intestinal ischemia. Textbook of Gastroenterology. Blackwell Publishing Ltd. 2009;2811–2830.

98. Cudnik MT, Darbha S, Jones J, Macedo J, Stockton SW, Hiestand BC. The diagnosis of acute mesenteric ischemia: a systemic review and meta-analysis. Acad Emerg Med. 2013;20:1087–1100.

99. Rahman SH, Ammori BJ, Holmfield J, Larvin M, McMahon MJ. Intestinal hypoperfusion contributes to gut barrier failure in severe acute pancreatitis. J Gastrointest Surg. 2003 Feb 1;7:26–36.

100. Graham JP, Lord PF, Harrison JM. Quantitative estimation of intestinal dilation as a predictor of obstruction in the dog. J Small Anim Pract. 1998;39:521–524.

101. Finck C, D'Anjou M-A, Alexander K, Specchi S, Beauchamp G. Radiographic diagnosis of mechanical obstruction in dogs based on relative small intestinal external diameters: small intestinal obstruction in dogs. Vet Radiol Ultrasound. 2014;55:472–479.

102. Hoey S, Drees R, Hetzel S. Evaluation of the gastrointestinal tract in dogs using computed tomography. Vet Radiol Ultrasound. 2013;54:25–30.

103. Tidwell AS, Penninck DG. Ultrasonography of gastrointestinal foreign bodies. Vet Radiol Ultrasound. 1992;33:160–169.

104. Sharma A, Thompson MS, Scrivani PV, et al. Comparison of radiography and ultrasonography for diagnosing small intestinal mechanical obstruction in vomiting dogs. Vet Radiol Ultrasound. 2011;52:248–255.

105. Shanaman MM, Hartman SK, O'Brien RT. Feasibility for using dual-phase contrast-enhanced multi-detector helical computed tomography to evaluate awake and sedated dogs with acute abdominal signs. Vet Radiol Ultrasound. 2012;53:605–612.

106. Oliveira CR, Mitchell MA, O'Brien RT. Thoracic computed tomography in feline patients without use of chemical restraint. Vet Radiol Ultrasound. 2011;52:368–376.

107. Oliveira CR, Ranallo FN, Pijanowski GJ, et al. The Vetmousetrap™: a device for computed tomographic imaging of the thorax of awake cats. Vet Radiol Ultrasound. 2011;52:41–52.

108. Fields EL, Robertson ID, Brown JC. Optimization of contrast-enhanced multidetector abdominal computed tomography in sedated canine patients. Vet Radiol Ultrasound. 2012;53:507–512.

109. Fields EL, Robertson ID, Osborne JA, Brown JC. Comparison of abdominal computed tomography and abdominal ultrasound in sedated dogs. Vet Radiol Ultrasound. 2012;53:513–517.

110. Manley R, Matthews AR, Morandi F, et al. Magnetic resonance imaging of the canine abdomen: effect of pulse sequence on diagnostic quality. Vet Radiol Ultrasound. 2013;54:253–262.

111. Shanaman MM, Schwarz T, Gal A, O'Brien RT. Comparison between survey radiography, B-mode ultrasonography, contrast-enhanced ultrasonography and contrast-enhanced multi-detector computed tomography findings in dogs with acute abdominal signs. Vet Radiol Ultrasound. 2013;54:591–604.

112. Tyrrell D, Beck C. Survey of the use of radiography vs. ultrasonography in the investigation of gastrointestinal foreign bodies in small animals. Vet Radiol Ultrasound. 2006;47:404–408.

113. Hayes G. Gastrointestinal foreign bodies in dogs and cats: a retrospective study of 208 cases. J Small Anim Pract. 2009;50:576–583.

114. Hobday MM, Pachtinger GE, Drobatz KJ, Syring RS. Linear *versus* non-linear gastrointestinal foreign bodies in 499 dogs: clinical presentation, management and short-term outcome. J Small Anim Pract. 2014 Nov;55:560–565.

115. Ellison GW. Complications of gastrointestinal surgery in companion animals. Vet Clin North Am Small Anim Pract. 2011 Sep;41:915–934.

116. Rademacher N, Schur D, Gaschen F, Kearney M, Gaschen L. Contrast-enhanced ultrasonography of the pancreas in healthy dogs and in dogs with acute pancreatitis. Vet Radiol Ultrasound. 2016;57:58-64.

117. Jones ID, Lamb CR, Drees R, Priestnall SL, Mantis P. Associations between dual-phase computed tomography features and histopathologic diagnoses in 52 dogs with hepatic or splenic masses. Vet Radiol Ultrasound. 2016;57:144-153.

118. Kutara K, Seki M, Ishikawa C, et al. Triple-phase helical computed tomography in dogs with hepatic masses. Vet Radiol Ultrasound. 2014;55:7-15.

119. Plonka AJ, Schentag JJ, Messinger S, et al. Effects of enteral and intravenous antimicrobial treatment on survival following intestinal ischemia in rats. J Surg Res. 1989;46:216-220.

APPENDIX A

LIST OF ABBREVIATIONS

1. CT – computed tomography
2. CEUS – contrast-enhanced ultrasound
3. HU – Hounsfield unit
4. ROI – region of interest
5. HCC – hepatocellular carcinoma
6. NASH – non-alcoholic steatohepatitis
7. IOUS – intra-operative ultrasound
8. VCAM-1 – vascular cell adhesion protein 1
9. ICAM-1 – intercellular adhesion molecule 1
10. PDH – pituitary-dependent hyperadrenocorticism
11. GST – glutathione S-transferase
12. IFABP – intestinal fatty acid binding protein
13. MRI – magnetic resonance imaging
14. TSE – turbo spin echo
15. FLASH GRE – fast low-angle shot gradient echo
16. HASTE – half-Fourier acquisition single-shot turbo spin echo
17. TIFF – tagged image file format